Check for updates

Received: 22 August 2023 | Revised: 27 December 2023 | Accepted: 5 January 2024

DOI: 10.1002/ces2.10201

International Journal of Ceramic Engineering & Science

REVIEW ARTICLE

Ceramic compositions for 5G devices containing niobium: A survey

Reginaldo Muccillo | **Eliana N. S. Muccillo**

Center of Science and Technology of Materials, Energy and Nuclear Research Institute, Sao Paulo, Brazil

Correspondence
Eliana N. S. Muccillo, Center of Science and Technology of Materials, Energy and Nuclear Research Institute, Av. Prof. Lineu Prestes 2242, Cidade Universitária, Sao Paulo, SP, Brazil.
Email: enavarro@usp.br

Funding information
CNEN; CDMF-CEPID; FAPESP, Grant/Award Number: 2013/07296-2; CNPq, Grant/Award Numbers: 302357/2018-1, 305557/2022-0

Abstract

The main dielectric properties of several ceramic materials having niobium in their composition, proposed to take part in 5G telecommunication devices, are reviewed. A preliminary basic presentation of 5G systems, the requirements for implementing their use, a concise review of the ceramic compositions containing niobium that have been studied thus far, and an evaluation of their performance are detailed. A survey is presented, including more than 80 different compositions containing niobium, focusing on key parameters, such as dielectric constant, quality factor, temperature coefficient, and sintering temperature. These parameters play a role for assessing the potential application of these ceramics in 5G devices.

KEYWORDS
5G, ceramics, dielectric properties, niobium compounds, wireless communication

1 | INTRODUCTION

Nowadays, wireless communication systems are continuously advancing, particularly for their application in mobile devices and satellite broadcasting, allowing access to previously inaccessible regions of the Earth and space satellite pathways. Ceramic materials play a vital role in this development, due to their favorable dielectric behavior, enabling their utilization in devices that require high-frequency response, such as resonators, antennas, and filters.[1–3] Furthermore, numerous ceramic compositions meet the essential requirements for their integration into communication system devices, including the availability of raw materials, straightforward synthesis techniques for obtaining suitable powders, low-temperature densification, and compatibility with metal electrodes during sintering, as well as mechanical reliability despite their small dimensions. The ongoing research focuses on electroceramics with minimal signal latency (no delays between transmitted and received signals), suitable dielectric constants, and extremely low (near-zero) temperature coefficients. Although 5G telecommunication devices have already been partially implemented, research efforts are underway looking for low-cost ceramic materials with enhanced properties.

1.1 | Brief historical overview

Wireless communication originated with analogic devices for 1G systems in 1980. In 1991, 2G systems were introduced, utilizing digital signals and incorporating technologies, such as GPRS (*General Packet Radio Service*) and EDGE (*Enhanced Data Rates for GSM Evolution*), which enabled devices to connect via the internet. In 2001, 3G systems were launched, offering higher data transfer rates and

This is an open access article under the terms of the Creative Commons Attribution License, which permits use, distribution and reproduction in any medium, provided the original work is properly cited.
© 2024 The Authors. *International Journal of Ceramic Engineering & Science* published by Wiley Periodicals LLC. on behalf of the American Ceramic Society.

exploiting dielectric materials with ultra-low loss tangent. The advent of 4G technology occurred in 2011, employing metalized dielectric ceramics as filters, allowing specific wave frequencies to be transmitted. Currently, there is a significant demand for communication devices operating in the 700 MHz−2.7 GHz range. Modern wireless communication requires even faster data transfers. 5G systems provide data transfer rate at least 10 times higher, low latency, and improved man-machine connectivity.[1–3] The 5G chipset market was estimated at US$ 490 million in 2018 and projected to reach US$ 10.9 billion by 2024.[4]

For communication systems operating in the microwave frequency range, dielectric ceramics with specific characteristics are required. These characteristics include: (1) high dielectric constant ($20 \leq \varepsilon_r \leq 35$) to allow for producing miniaturized devices; (2) high-quality factor (Qxf ≥ 100 000 GHz), to improve signal quality and to allow for frequency tuning, allowing the use of multiple channels at different frequencies; (3) near-zero temperature coefficient (TCF or $\tau_f \sim 0 \pm 2$ ppm/°C) at the resonance frequency: the dielectric response should remain constant despite ambient temperature variations, such as the transition from winter to summer (−30°C to + 30°C), or the range of −55°C to + 85°C, depending on the satellite or space vehicle's position; and (4) sintering temperature lower than 950°C, to facilitate the deposition of silver electrodes and ensure chemical compatibility between the dielectric material and the electrodes.[5]

Many research reports in this field are primarily concerned with finding cost-effective materials and establishing correlations between microstructural characteristics and dielectric properties. Dielectric ceramics with various parameters find applications based on their specific characteristics: (1) high dielectric constant: these ceramics are advantageous as they can reduce signal transmission delays; (2) high-quality factors: these ceramics are beneficial in reducing power losses within the system; (3) near-zero temperature coefficients: these ceramics contribute to improved thermal stability of the system, ensuring minimal variation in dielectric constant under temperature changes; and (4) sintering temperature below 950°C: enables the application of these ceramics for the utilization of low-cost silver electrodes, providing cost-effective solutions. Exploring these parameters and their correlations with microstructural characteristics, researchers aim to identify and develop dielectric ceramics that meet specific requirements for various applications.[6,7]

The operation frequencies of 5G communication systems are higher than those used in 4G systems. They include 3.5, 3.7, and 4.7 GHz frequencies, and the 26, 28, and 39 GHz millimeter waves (wavelength of the order of mm).[1–3]

Data extracted from the Web of Science database using the keywords "5G" with "ceramics" and "5G" with "Nb" show an exponential increase in the number of publications and citations starting from 2016 for both sets of keywords, indicating a growing interest and research activity in these areas.

1.2 | Ceramics for 5G

Ceramics used in 5G applications are typically polycrystalline inorganic compounds, either as sintered pellets or thin and thick films. Their primary function is to serve as dielectrics operating at frequencies in the GHz range. Significant research efforts have been dedicated to exploring the use of dielectric ceramics in 5G (and more recently for 6G) for communication devices.[8] These are the dielectric properties that have to be evaluated: the dielectric constant, which determines the material's ability to store electrical energy; the quality factor, which reflects the material's efficiency in transmitting and storing energy; and the temperature coefficient, which indicates the material's sensitivity to temperature changes. Additionally, the sintering temperature is also important to ensure compatibility with the integration of electronic components through metal electrodes.[8,9]

Defining those parameters:

- dielectric constant (ε_r): is the ratio of the dielectric capacitance to that of the vacuum. It expresses the ability of the dielectric to store energy when submitted to an electric voltage. That ability is usually ascribed to electric dipoles in the crystalline structure of the compound. One simple example of a dipole is the Y^{3+}-O^{2-}-Y^{3+} complex in yttria-stabilized zirconia. Higher values mean the possibility of using ceramic pieces with small dimensions, decreasing the size of devices and also the cost/weight ratio. The dielectric constant is known to depend on the polarizability.[10,11]
- the quality factor (Qxf) of a dielectric material is defined as the product of the standing time and the resonance frequency. It represents the duration for which the resonance oscillation (wireless signal) of the dielectric remains active. A higher Qxf indicates better frequency selectivity and a longer operation time at the desired frequency. The quality factor depends on both intrinsic and extrinsic losses. Intrinsic losses are associated with modes of lattice vibration within the material, while extrinsic losses are related to lattice defects, such as oxygen vacancies, porosity, and secondary phases. The quality factor is particularly significant in applications such as long-distance medical surgeries, where the instantaneous response of the surgeon is critical during the manipulation of surgical devices. A higher quality factor ensures improved frequency selectivity and

25783270, 0, Downloaded from https://ceramics.onlinelibrary.wiley.com/doi/10.1002/ces2.10201 by CAPES, Wiley Online Library on [19/01/2024]. See the Terms and Conditions (https://onlinelibrary.wiley.com/terms-and-conditions) on Wiley Online Library for rules of use; OA articles are governed by the applicable Creative Commons License

stability, contributing to enhanced performance and precision in such applications.
- the temperature coefficient (τ_f) is a measure of how the dielectric constant varies with temperature. A near-zero value indicates better thermal stability, making it more suitable for applications in devices that may be located at regions of varying temperature, for example, desert areas (northern Africa), polar regions (northern Hemisphere), or satellites.
- the sintering temperature (T_s) refers to the temperature required to obtain a dense ceramic compound, usually prepared by solid-state reaction among the constituents' oxides, to achieve a solid solution and/or densification. Lower values mean easiness to deposit low-cost metal electrodes, usually silver, which melts at 960°C. Lower sintering temperatures can help in reducing the energy consumption and cost associated with the sintering process. Operating at lower temperatures can save energy and make the manufacturing process more cost-effective.

It is widely acknowledged that the performance of ceramics in 5G devices is highly dependent on their microstructure. The dielectric constant ε_r depends on the relative density, due to the contribution of the porosity and of the unit cell volume that defines the polarizability. The quality factor Qxf depends on the binding energy of the (cation)-(oxygen ion) bond, as well as the average grain size. Microstructural features are considered due to the dependence of the dielectric properties on bulk density, porosity, average grain size, grain size distribution, and secondary phases.[12] Understanding and controlling these microstructural aspects are essential for optimizing the performance of these materials in 5G applications. Earlier studies on ceramic materials for 3G technology highlighted the relevance of the structure and microstructure on the dielectric properties. In the sequence, as an example, a brief review on complex perovskite ceramics for use in 5G telecommunication devices is given.

Ceramic materials with perovskite structure were fully investigated due to their excellent dielectric properties. The complex perovskite $BaZn_{1/3}Ta_{2/3}O_3$ is an example, with ε_r = 30, Qxf = 150 000, and τ_f = 0 ppm/°C. Substitution of Ta_2O_5 for Nb_2O_5 was promptly performed in these complex perovskites, to improve the cost effectiveness of the dielectric ceramics. Moreover, Ta_2O_5-based complex perovskite ceramics usually require high sintering temperatures to achieve good densification. The $BaZn_{1/3}Nb_{2/3}O_3$ (BZN) ceramic exhibited ε_r = 38, Qxf = 90 000, and τ_f = 30 ppm/°C.[13] Attempts have been made to decrease the value of τ_f changing the compositional variation. The composite $0.9[(Zn_{0.60}Co_{0.40})_{0.33}Nb_{0.67}]O_3$-$0.1Ba(Ga_{0.5}Ta_{0.5})O_3$, 0.9BCZN-0.1BGT, for example, showed ε_r = 35, Q = 32 000, f = 3.056, and τ_f = 0 ppm/°C.[14]

It was shown that the dielectric properties of complex perovskite structure such as $AB'_{1/3}B''_{2/3}O_3$ are strongly dependent on the cationic ordering, promoting a drastic decrease of the dielectric losses with increasing the degree of ordering. The 1:2 ordering of B-site cations is formed due to differences in size and valence of the two B-site ions. In this context, nonstoichiometry was also shown to play a role in the dielectric properties. The addition of up to 0.02 mol% $Ba_3W_2O_9$ to BZN increased the concentration of cation vacancies and decreased the sintering temperature due to liquid phase formation, resulting in highly dense ceramics. In addition, Zn vacancies were reported to accelerate the ordering process. These factors accounted for the high Qxf value (118 500) obtained at 8 GHz for x = 0.007.[15] The relationship between ceramic processing and deviation from stoichiometry was also reported for $BaCo_{1/3}Nb_{2/3}O_3$ (BCN); although nonstoichiometry was barely detected, its influence was notorious on the extrinsic electrical conductivity.[16] $Ba(Mg_{1/3-x}Nb_{2/3})O_3$ (BMN) compositions with $0 \leq x \leq 0.04$, prepared by the solid-state reaction method and sintered at 1450°C for 4 h, showed an increase of the cation ordering, and relative density for small Mg deficiency. The highest Q value achieved was 12 000 at 8 GHz for x = 0.02.[17]

It was clear from those previous studies that the processing and sintering profiles, besides partial substitutions, are important experimental procedures to tune the dielectric properties of ceramics.

Numerous ceramic compositions have been described as suitable for use in 5G devices: niobates, titanates, phosphates, silicates, molybdates, tantalates, and tungstates. In this survey, the focus is specifically on compositions containing niobium, and their main properties that are relevant for 5G devices. By narrowing down the investigation to niobium-containing compositions, the survey aims to highlight and analyze the main properties of these specific ceramics that are important for their application in 5G devices. Figure 1 shows a schematic view of the main issues focused on this survey.

This focused approach allows for a deeper understanding of the specific characteristics and performance requirements of niobium-based ceramic materials in the context of 5G technology.

2 | CERAMIC COMPOSITIONS FOR 5G DEVICES

Unless stated otherwise, all ceramic compounds here reviewed were synthesized by the solid-state reaction route or solid-state synthesis method. This involves the mixing of precursor oxides, followed by thermal treatment (calcination) in either resistive or microwave furnaces to achieve a solid solution. However, making direct

25783270, 0, Downloaded from https://ceramics.onlinelibrary.wiley.com/doi/10.1002/ces2.10201 by CAPES, Wiley Online Library on [19/01/2024]. See the Terms and Conditions (https://onlinelibrary.wiley.com/terms-and-conditions) on Wiley Online Library for rules of use; OA articles are governed by the applicable Creative Commons License

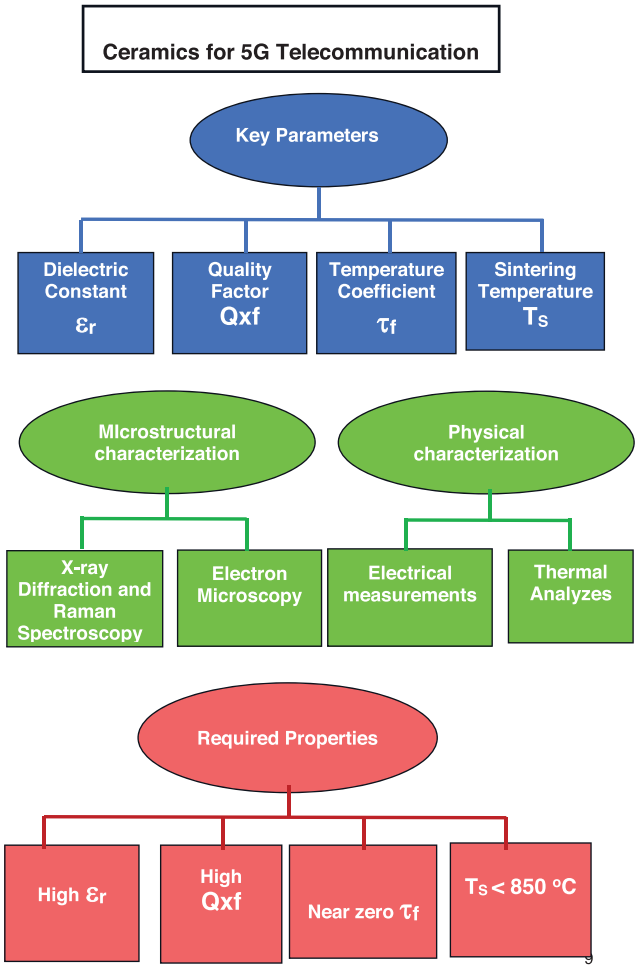

FIGURE 1 Scheme of the main topics addressed in this survey on ceramics for 5G telecommunication devices containing niobium: key parameters, microstructural and physical characterizations, and required properties (see text for details).

comparisons among the reported results can be challenging, primarily due to variations in experimental conditions during sample measurements. Moreover, the processing parameters varied, for example, the milling time, type and concentration of organic binders, calcination and sintering profiles, and other processing conditions, leading to different microstructures.

Nanosized powders are often synthesized using solution methods and are known to exhibit enhanced sinterability. However, these solution methods can be time-consuming and not cost-effective for large-scale technological applications. Then, the addition of both glass and nonglass sintering aids became common practice to reduce the sintering temperature required for the densification of ceramic compositions. The sintering aids usually facilitate the bonding between particles and enhance the mobility of atoms during the sintering process.

Initial studies on lithium niobates were conducted on cubic rock salt structures, including Li_3NbO_4 and $Li_3Mg_2NbO_6$. It was found that these ceramics exhibit the dielectric constant in the range from 10 to 25; the Qxf value increased in the sequence Li_3NbO_4 and $Li_3Mg_2NbO_6$. Besides the relatively high Qxf values of compounds with rock salt structure, the τ_f value is not easily adjusted as for perovskite ceramics. In the latter, the τ_f may be tuned by changing the tilting angle of the corner-shared oxygen octahedrons. In rock salt structure ceramics, the edge-shared oxygen octahedrons are not expected to tilt in the same way. Good microwave dielectric properties were obtained for $Li_3Mg_2NbO_6$: $\varepsilon_r = 16.8$, Qxf = 79 643 GHz, and $\tau_f = -27.2$ ppm/°C.[18]

A mixture of Li_3NbO_4 was co-fired with 20 wt.% Ag at 900°C, while pure Li_3NbO_4 was sintered in the 870–970°C range. The density of pure ceramic increased to ~97% as the sintering temperature reached a near steady-state at ~930°C. The values of Qxf and ε_r also increased up to 930°C, whereas τ_f remained unchanged with the dwell temperature. The grain sizes observed in the ceramics were relatively small (1–2 μm), compared to other compositions. The optimal microwave dielectric properties were achieved for specimens sintered at 930°C, with $\varepsilon_r = 15.8$, Qxf = 55 009 GHz at 8.99 GHz, and $\tau_f = -49$ ppm/°C.[5]

In the next two sections, $Li_3Mg_2NbO_6$ and other Li-based compositions will be described.

2.1 | $Li_3Mg_2NbO_6$-based compositions

Reports on the synthesis of $Li_3Mg_2NbO_6$ date back to 1982.[19] In recent years, the dielectric properties of lithium and magnesium niobates were consistently reported.[20–22] Improvement of the dielectric properties was obtained with substitutional doping at Mg and Nb sites, for example, with Cu,[10] Ta,[11] Co,[23] Ca,[24,25] Ni,[25] Mn,[25] Sn,[26] Zn,[25,27,28] Sb,[29] V,[30] Mo,[31] W,[32] Ti,[33,34] co-doping with W-Li/Mg/Al/Ti,[35] co-doping with Li-Ti,[36] and using B_2O_3,[37] TiO_2,[38] $MgO+B_2O_3+SiO_2$,[39] and $Li_2O+B_2O_3+SiO_2+CaO+Al_2O_3$[40] sintering aids.

Early studies on $Li_3Mg_2NbO_6$ were conducted to verify the effects of partial substitutions of Mg^{2+} and Zn^{2+} into the Li^+ site of Li_3NbO_4. Extensive solid solutions were expected to occur, due to the similarity in ionic radii between Li^+, Mg^{2+}, and Nb^{5+}, as well as the similarity between the crystalline structure of Li_3NbO_4 and MgO. The specimens were sintered in the 1200–1350°C range. The crystal structure of $Li_{3-3x}M_{4x}Nb_{1-x}O_4$ ($0 < x \leq 0.9$), with M = Mg, Zn, was characterized by X-ray diffraction and Raman spectroscopy. For x = 0, the X-ray diffraction pattern of Li_3NbO_4 exhibited a cubic ordered structure along with a secondary phase, $Nb_{12}O_{29}$, which is characteristic of Nb reduction. The presence of this phase was attributed to the loss of Li by evaporation during the thermal treatment at high temperatures.[41] The addition of Mg ($0.01 \leq x \leq 1/3$) promoted the stabilization of a disordered

25783270, 0, Downloaded from https://ceramics.onlinelibrary.wiley.com/doi/10.1002/ces2.10201 by CAPES, Wiley Online Library on [19/01/2024]. See the Terms and Conditions (https://onlinelibrary.wiley.com/terms-and-conditions) on Wiley Online Library for rules of use; OA articles are governed by the applicable Creative Commons License

cubic structure without the formation of secondary phases. On the other hand, the addition of Zn did not result in solid solution formation or the creation of a new compound. The X-ray diffraction patterns showed the presence of Li_3NbO_4 and ZnO throughout the entire composition range. The dielectric constant (ε_r) values for the studied compositions were in the 16.3–16.8 range. The quality factor varied from 32 765 (x = 0, sintered at 1150°C/2 h) to 85 160 GHz (x = 0.2, sintered at 1300°C/2 h), and the temperature coefficient (τ_f) from −22 (x = 1/3, sintered at 1300°C/2 h) to −45 ppm/°C (x = 0, sintered 1150°C/2 h).[41]

2.2 | Pure $Li_3Mg_2NbO_6$

These ceramics, considered to be a promising candidate for devices operating in the millimeter wavelength spectral region, were prepared either pure,[8,19] or with the addition of dopants or sintering aids[10,11,23–40] for improving their properties or decreasing the sintering temperature. The dielectric properties of the pure compound sintered at 1250°C were ε_r = 16.8, Qxf = 79 643 GHz, and τ_f = −27.2 ppm/∘C.[35] Stoichiometric $Li_3Mg_2NbO_6$ with submicron particle size (~222 nm) was obtained by high-energy milling. High relative density (~96%), ε_r ~18, Qxf ~51 870 GHz, and τ_f ~ −23 ppm/°C were obtained for specimens sintered at 950°C,[22] evidencing the beneficial effect of the synthesis by chemical methods on densification.

$Li_{3+x}Mg_2NbO_6$ (x = 0–0.08): excess Li in the base composition allowed for a small decrease in the sintering dwell temperature (~1250 to ~1150°C), and significant increase in the quality factor (~79 000 to ~150 000). The lattice parameter and cell volume increased, indicating that Li was incorporated into the crystal lattice. The bulk density and the dielectric constant were higher than those of the stoichiometric composition. The grain size increased up to x = 0.04 in the $Li_{3+x}Mg_2NbO_6$. The optimized parameters, assumed to be due to Li compensation owing to lithium volatilization during sintering, were ε_r ~16, Qxf ~150 000 GHz, and τ_f ~ −29 ppm/°C (x = 0.04).[20]

2.2.1 | $Li_3Mg_{2-x}A_xNbO_6$ partial substitution for the Mg^{2+} ion

In general, ceramics containing partial substitutions in the Mg^{2+} site exhibited dielectric constant values in the 14–16 range. However, the quality factor and temperature coefficient varied considerably, influenced by factors such as sintering temperature, density, and other variables.

Co-doping: $Li_3(Mg_{1-x}Co_x)_2NbO_6$ ($0.00 \le x \le 0.10$)
The Qxf values of samples sintered at 1300°C/4 h increased from 91 600 GHz for x = 0 to 127 600 GHz for x = 0.02. No secondary phases were detected, and all compositions exhibited orthorhombic structure. The microwave dielectric properties were ε_r = 15.22, Qxf = 127 600 GHz, and τ_f = −3.64 ppm/°C.[23]

Ca-doping: $Li_3(Mg_{1-x}Ca_x)_2NbO_6$ ($0.02 \le x \le 0.08$)
Ceramics were found in single phase with orthorhombic structure after sintering at 1060–1220°C/6 h. A more homogeneous microstructure with grain sizes in the 20–35 μm range was obtained after sintering at 1140°C/6 h, for x = 0.04, with ε_r ~16.81, Qxf ~98 000 GHz, and τ_f ~ −25.8 ppm/°C.[24] Based on experimental data, it was concluded that ε_r and Qxf are mainly related to density. LiF was used as a sintering aid to reduce the dwell temperature. The optimal microwave dielectric properties, ε_r = 15.85, Qxf = 98 012 GHz, and τ_f = −28.6 ppm/°C, were obtained after sintering at 900°C/6 h with 6 wt.% LiF.[24] Another work, doping with 0.05 mol Ca^{2+}, yielded ε_r = 15.62, Qxf = 96 160 GHz (at 8.971 GHz), and τ_f = −18.49 ppm/°C. The Qxf and ε_r values were comparatively lower for Mn^{2+} substitution in the Mg^{2+} site (52 700 GHz and 12.97, respectively) with τ_f = −20.13 ppm/°C.[25] All the prepared compositions had rock salt structure.

Cu-doping: $Li_3Mg_{2-x}Cu_xNbO_6$ ($x = 0–0.04$)
These ceramics were shown to achieve high relative density after sintering at 1000–1120°C, with high value of ε_r (15.75), Qxf = 92 134 GHz (9.86 GHz), and near-zero τ_f = −2 ppm/°C for x = 0.02.[10] In this case, ε_r was shown to correlate with the polarizability, whereas Qxf was influenced by the packing fraction.

Sn-doping: $Li_3Mg_{2-x/3}Sn_xNb_{1-2x/3}O_6$
Simultaneous partial substitution on Mg^{2+} and Nb^{5+} sites were also investigated with Sn^{4+} doping in $Li_3Mg_{2-x/3}Sn_xNb_{1-2x/3}O_6$ ($0 \le x \le 1.5$).[26] For x value up to 0.1, the compositions exhibited the typical orthorhombic structure of $Li_3Mg_2NbO_6$, which changed to the characteristic cubic phase of $Li_2Mg_3SnO_6$ for $x \ge 0.7$. The optimal dielectric parameters were found in a mixed orthorhombic-cubic (x = 0.3) phase field for specimens sintered at 1290°C with ε_r = 15.9, Qxf = 118 700 GHz (f = 7.99 GHz), and τ_f = −32.9 ppm/°C. Nevertheless, the temperature stable properties were obtained for x = 1.2 (ε_r = 11.64, Qxf = 83 100 GHz at f = 10.30 GHz, and τ_f = 3.9 ppm/°C).[26]

Zn-doping: $Li_3(Mg_{1-x}Zn_x)_2NbO_6$ ($0 < x < 0.1$)
These ceramics exhibited the following microwave dielectric properties: ε_r = 17.2, Qxf = 142 331 GHz, τ_f = 23.2 ppm/°C for x = 0.08 and sintered at 1120°C/4 h. Addition of a small amount of sintering aid, 0.5 wt.% ($0.17Li_2O$-$0.83V_2O_5$), allowed for sintering at 925°C/2 h

25783270, 0, Downloaded from https://ceramics.onlinelibrary.wiley.com/doi/10.1002/ces2.10201 by CAPES, Wiley Online Library on [19/01/2024]. See the Terms and Conditions (https://onlinelibrary.wiley.com/terms-and-conditions) on Wiley Online Library for rules of use; OA articles are governed by the applicable Creative Commons License

with the following microwave dielectric properties: $\varepsilon_r = 14$, Qxf = 83 395 GHz, and $\tau_f = 37.2$ ppm/°C.[27] X-ray diffraction evidenced that $Li_3Mg_2NbO_6$ was the main crystalline phase, besides minor amounts of secondary phases such as NbO and $Mg_4Nb_2O_9$, after sintering at 1200°C. Optimal dielectric properties were obtained for x = 0.04 with $\varepsilon_r = 16.3$, Qxf = 93 100 GHz, and $\tau_f = -34.1$ ppm/°C. Adding Li^+ and Zn^{2+}, the composition $Li_{3.04}Mg_{1.96}Zn_{0.04}Nb_{0.96}Ti_{0.04}O_6$ yielded $\varepsilon_r = 16.3$, Qxf = 93 100 GHz, and $\tau_f = -34.1$ ppm/°C.[28]

$Li_3(Mg_{0.95}A_{0.05})_2NbO_6$ ($A = Ca^{2+}, Ni^{2+}, Zn^{2+}, Mn^{2+}$)
These ceramic compositions were sintered at 1120–1240°C/4 h in air. X-ray diffraction evidenced solid solution formation with rock salt structure; the following parameters were obtained: A = Ca^{2+}, $\varepsilon_r = 15.62$, Qxf = 96 160 GHz, and $\tau_f = -18.47$ ppm/°C; A = Ni^{2+}, $\varepsilon_r = 15.24$, Qxf = 84 810 GHz, and $\tau_f = -23.08$ ppm/°C; A = Zn^{2+}, $\varepsilon_r = 15.39$, Qxf = 82 170 GHz, and $\tau_f = -18.57$ ppm/°C; A = Mn^{2+}, $\varepsilon_r = 12.97$, Qxf = 52 700 GHz, and $\tau_f = -20.13$ ppm/°C.[25] In this case, Qxf and τ_f varied similarly to the packing fraction and to the Mg site bond valence, respectively. These results show that Ca^{2+} and Zn^{2+} exert almost the same effect on the dielectric properties.

2.2.2 | $Li_3Mg_2Nb_{1-x}A_xO_6$ partial substitution for the Nb^{5+} ion

Regarding partial substitutions in the Nb^{5+} site with both isovalent and aliovalent cations, interesting characteristics were observed. In particular, the dielectric constant remained similar (~16) with the substitution of Nb^{5+} for M^{5+} cations (M^{5+} = V, Sb, and Ta). The addition of Ta promoted grain growth and increase of the density, contributing to decrease the fraction of grain boundaries and, consequently, to reduce the dielectric loss. However, a significant increase of the Qxf value was observed for V^{5+} (~131 000 GHz) and near-zero τ_f for Ta^{5+} (−4.5 ppm/°C) substitutions. The sintering temperature was relatively lower for V^{5+} addition (900°C) and higher for Ta^{5+} addition (1150°C).[11,30]

Sb-doping: $Li_3Mg_2(Nb_{1-x}Sb_x)O_6$ ($0.02 \le x \le 0.08$)
Ceramic compositions were prepared by calcination of stoichiometric amounts of lithium carbonate and magnesium, niobium, and antimony oxides, pressing into pellets and sintering at 1075–1200°C/6 h. Substitution of Sb^{5+} in the Nb^{5+} site provided a large increase of the quality factor and grain growth. The $Li_3Mg_2(Nb_{0.94}Sb_{0.06})$ sintered at 1150°C/6 h showed 15.79, 94 487 GHz, and −24.53 ppm/°C for the dielectric constant ε_r, the quality factor Qxf, and the temperature coefficient τ_f, respectively.[29]

V-doping: $Li_3Mg_2Nb_{1-x}V_xO_6$ ($x = 0.02, 0.04, 0.06, 0.08$)
$Li_3Mg_2NbO_6$ was mixed to vanadium oxide (xV_2O_5, $0.25 \le x \le 1.25$ wt.%) to reduce the sintering temperature. Specimens sintered at 925°C/4 h exhibited a dense microstructure with grain sizes in the ~8 to ~11 μm range. The ideal concentration of V_2O_5 was 1 wt.%, with ε_r ~15.1, Qxf = 91 000 GHz, and $\tau_f \sim -24$ ppm/°C.[21] The Qxf value was influenced by the relative density and the average grain size.

Ta-doping: $Li_3Mg_2Nb_{1-x}Ta_xO_6$
Ceramics with substitution in the Nb^{5+} site for Ta^{5+}, and its effect on the structural characteristics and microwave dielectric performances was investigated. The composition sintered at 1100°C and with x = 0.02 displayed the microwave dielectric properties: $\varepsilon_r = 15.58$, Qxf = 113 000 GHz, and $\tau_f = -4.5$ ppm/°C. Specimens containing partial substitution in the Nb^{5+} site for Ta^{5+} exhibited a high-quality factor for x = 0.03, with an average grain size of ~10 μm.[11] The temperature coefficient τ_f was shown to be impacted by the NbO_6 octahedral distortion and Nb-O bond valence.

Mo-doping: $Li_3Mg_2(Nb_{(1-x)}Mo_x)O_{6+x/2}$ ($0 \le x \le 0.08$)
Substitution of Mo^{6+} in the Nb^{5+} site modified the grain size from 50–90 (x = 0) to 10–20 μm (x = 0.8) after sintering at 1200°C. The quality factor increased, with maximum value at x = 0.02 (116 266 GHz), and then decreased, whereas τ_f increased with increasing Mo content from ~ −20 to ~ −16 ppm/°C.[31] The ionic radius of Mo^{6+} is smaller than that of Nb^{5+} and a shift of the diffraction peaks toward higher angles was observed. As in other dielectric ceramics, the Qxf value was closely related to specimen density and bond valence.

W-doping: $Li_3Mg_2Nb_{1-x}W_xO_{6+x/2}$
The introduction of W^{6+} in the Nb^{5+} site promoted grain growth and increase of the density achieving > 96% for x = 0.06, after sintering at 1175°C.[32] In the case of substitution of M^{6+} (M^{6+} = Mo, W) for Nb^{5+}, the dielectric properties were similar for sintering at 1200°C[31] and 1175°C[32] with ε_r 15–16, Qxf in the 116 266–124 187 GHz range, and τ_f of −15.82 to −18.28 ppm/°C. The quality factor was found to be influenced by the average bond valence and the density.

Ti-doping: $Li_{3+x}Mg_{2-2x}Nb_{1-x}Ti_{2x}O_6$ ($0 \le x \le 1$)
Several reports may be found concerning Ti-doping. Substitution of Ti^{4+} in the Nb^{5+} site, $Li_3Mg_{2-x/3}Nb_{1-2x/3}Ti_xO_6$ ($0 \le x \le 0.6$), was investigated from a structure point of view. A disordered cubic structure without secondary phases was obtained in the $0.12 \le x \le 0.38$. The Qxf value increased

25783270, 0, Downloaded from https://ceramics.onlinelibrary.wiley.com/doi/10.1002/ces2.10201 by CAPES, Wiley Online Library on [19/01/2024]. See the Terms and Conditions (https://onlinelibrary.wiley.com/terms-and-conditions) on Wiley Online Library for rules of use; OA articles are governed by the applicable Creative Commons License

(82 338–125 357 GHz) with increasing x from 0 to 0.4, after sintering at 1260°C, with ε_r ~15 and $\tau_f = -31.7$ ppm/°C.[42] The main effect of partial substitution of Ti^4 in the Nb^{5+} site was to increase considerably the quality factor. A full range of solid solutions were found between $Li_3Mg_2NbO_6$ and Li_2TiO_3 with no trace of impurities.[34] The multicomponent $Li_{3+x}Mg_{2-2x}Nb_{1-x}Ti_{2x}O_6$ exhibited high Qxf value (128 600 GHz) at x = 0.2 after sintering at 1250°C, with ε_r ~16 and $\tau_f \sim -30.4$ ppm/°C. Temperature stable properties were found for x = 0.9 with $\varepsilon_r = 20.4$, Qxf = 90 300 GHz (f = 7.9 GHz), and $\tau_f = 2.9$ ppm/°C.[34] In another study, the effect of Ti^{4+} with ionic radius (0.605 Å) similar to that of Nb^{5+} (0.64 Å) was studied for x up to 0.10 in $Li_3Mg_2Nb_{1-x}Ti_xO_{6-x/2}$, after sintering at 1150°C. The grain sizes obtained were comparatively small (typically ~10 μm), with ε_r ~15.9, Qxf = 131 000 GHz, and $\tau_f = -26.8$ ppm/°C.[33]

Efforts to enhance the properties of dielectric ceramics have been undertaken also through the strategy of co-doping.[35,36]

Co-doping with W and Li/Mg/Al/Ti

The studied compositions, sintered at 1150°C/4 h, yielded the following values for ε_r, Qxf, and τ_f: $Li_3Mg_2Nb_{0.96}(Li_{1/5}W_{4/5})_{0.04}O_6$: 13.9806, 114 781, −22.33; $Li_3Mg_2Nb_{0.96}(Mg_{1/4}W_{3/4})_{0.04}O_6$: 13.8022, 105 879, −21.19; $Li_3Mg_2Nb_{0.96}(Al_{1/3}W_{2/3})_{0.04}O_6$: 13.7253, 102 760, −23.11; $Li_3Mg_2Nb_{0.96}(Ti_{1/2}W_{1/2})_{0.04}O_6$: 14.2356, 128 838, −21.12[35]; $Li_3Mg_2Nb_{0.96}W_{0.04}O_6$: 16.8, 79 643, 27.2. No secondary phases were observed by X-ray diffraction, but a shift toward a higher angle in the diffraction peaks. Partial substitutions of W^{6+} in the Nb^{5+} site and Li^+, Mg^{2+}, Al^{3+}, and Ti^{4+} in the complex $Li_3Mg_2Nb_{0.96}(M_xW_{1-x})_{0.04}O_6$ composition revealed single-phase ceramics up to x = 0.04. The Qxf value was higher for sintering temperatures of 1150°C/4 h with relative densities ~96%. The highest value of Qxf (128 838 GHz) was obtained for M = Ti^{4+}. The τ_f values varied from −21.12 to −27.2 ppm/°C.[35] The quality factor increased linearly with increasing the average bond valence.

Co-doping with (Li^+/Ti^{4+})

$Li_{3.06}Mg_2Nb_{0.94}Ti_{0.06}O_6$ ceramics sintered at 1025°C/4 h, prepared with excess Li along with partial substitution of Ti^{4+} in the Nb^{5+} site resulted in suitable values of the dielectric constant (~14), quality factor (154 113 GHz), and τ_f (~ −2 ppm/°C), after sintering at 1025°C.[36] These results are further evidence that excess Li is beneficial to increase the quality factor. Moreover, the co-doping with Ti in the Nb site was very effective to achieve a near-zero τ_f, which varied in a similar way as the bond energy.

2.2.3 | With sintering aids

To reduce the sintering temperature, several reports have focused on the use of sintering aids. Boron oxide (B_2O_3) and boron-based glasses have been employed for this purpose.[37–40] A complex glass based on Li_2O-B_2O_3-SiO_2-CaO-Al_2O_3 (LBSCA) was also incorporated to $Li_3Mg_2NbO_6$.[40]

B_2O_3 adding: $Li_3Mg_2NbO_6$ + x wt.% B_2O_3

Compounds, prepared by the solid-state method, had the sintering temperature reduced to 925°C/4 h. The dielectric constant and the quality factor varied according to the bulk density. Boron oxide added in small amounts (x = 0.05–1.5 wt.%) allowed for achieving 92% relative density after sintering at 950°C and promoted grain growth. Nevertheless, a secondary phase was detected by X-ray diffraction and observed on scanning electron microscopy micrographs. The quality factor value was shown to be influenced by the amount of the sintering aid and sintering temperature and τ_f varied from ~ −16 to ~ −22.5 ppm/°C with increasing amounts of B_2O_3. The microwave dielectric properties $\varepsilon_r = 14.0$, Qxf = 67 451 GHz, $\tau_f = -16.82$ ppm/°C were obtained for $Li_3Mg_2NbO_6$ −0.1 wt.% B_2O_3 ceramics sintered at 925°C/4 h.[37]

LBBS adding: $Li_3Mg_2NbO_6$-0.1TiO_2

These ceramics were synthesized with the addition of Li_2O-B_2O_3-Bi_2O_3-SiO_2 glass. The glass addition allowed for reducing the sintering temperature of $Li_3Mg_2NbO_6$-0.1TiO_2 to 900°C. A secondary phase (MgO) was detected by X-ray diffraction technique and τ_f shifted toward negative values. In this case, the dielectric constant ($\varepsilon_r = 16$) did not change significantly, the Qxf value was 42 648 GHz, and a near-zero $\tau_f \sim -1$ ppm/°C was obtained.[38]

MBS adding: $Li_3Mg_2NbO_6$

(0.1–2.0 wt.% MBS: 42 MgO, 45 B_2O_3, 13 SiO_2) was obtained by calcination at 1050°C/4 h of stoichiometric amounts of lithium carbonate and magnesium and niobium oxides. Pellets obtained with an addition of 0.5 wt.% MBS glass were sintered at 925°C/4 h achieving 95% of relative density. The microwave dielectric properties were $\varepsilon_r = 14.5$, Qxf = 80 759 GHz, and $\tau_f = -20.7$ ppm/°C.[39]

LBSCA adding: $Li_3Mg_2NbO_6$

Ceramics with an addition of LBSCA glass were prepared with 52.45 Li_2O:31.06 B_2O_3:11.99 SiO_2:2.25 CaO:2.25 Al_2O_3 at 1000°C/4 h. The dielectric ceramic with 0.5 wt.% of the glass additive sintered at 925°C/4 h and showed $\varepsilon_r = 15.16$, Qxf = 90 557 GHz, and $\tau_f = -16.22$ ppm/°C. The sintered density reached a maximum value (~96% for 0.25 wt.%

25783270, 0, Downloaded from https://ceramics.onlinelibrary.wiley.com/doi/10.1002/ces2.10201 by CAPES, Wiley Online Library on [19/01/2024]. See the Terms and Conditions (https://onlinelibrary.wiley.com/terms-and-conditions) on Wiley Online Library for rules of use; OA articles are governed by the applicable Creative Commons License

LBSCA) for a sintering dwell temperature of 950°C. No secondary phases were detected by X-ray diffraction after sintering at 925°C. Increase of the sintering temperature to 975°C resulted in abnormal grain growth in specimens containing 0.5 wt.% of LBSCA.[40]

B_2O_3-CuO with addition of $[Li_2Ti_{0.98}Mg_{0.02}O_{2.96}F_{0.04}$–1 wt.% Nb_2O_5 (LTMN)]-x$Li_3Mg_2NbO_6$, $0 \leq x \leq 0.1$

Ceramics were prepared by solid-state synthesis and the sintering temperature was lowered from 1120°C to 750°C by adjusting the mass ratio of B_2O_3–CuO (BC), with a relatively low eutectic point. The dielectric properties (ε_r ~24.44, Qxf ~60 574 GHz, and τ_f ~22.8 ppm/∘C) were obtained in BC-modified LTMN ceramics sintered at 790°C.[43]

In general, sintering additives were found to be effective to reduce the sintering temperature, without compromising the dielectric properties of the ceramics.

2.2.4 | Other compositions containing lithium

(1−x) Li_3NbO_4−x $CaTiO_3$ ($0.1 \leq x \leq 0.3$)

The composites were prepared, and the dielectric properties of lithium niobate changed according to calcium titanate additions. X-ray diffraction showed the Li_3NbO_4 cubic structure and $CaTiO_3$ perovskite structure. High density and high ε_r values were achieved after sintering at 1250°C. The temperature coefficient of resonant frequency could be adjusted to near-zero. Particularly, for x = 0.15, the ceramic sintered at 1025°C/4 h exhibited ε_r = 21.9, Qxf = 24 900 GHz, and τ_f = 5.6 ppm/°C.[44]

Li_3MgNbO_5

The composition with rock salt structure was synthesized by the two-step sintering method. The phase purity of Li_3MgNbO_5 was validated by X-ray diffraction in specimens sintered in the 1200–1280°C. The grain size increased from ~11 to ~40 μm according to the sintering temperature. Optimal properties (ε_r = 16.2, Qxf = 96 796 GHz, and τ_f = −24.8 ppm/°C) were obtained for sintering at 1260°C.[45] Adjustment of the temperature coefficient of resonant frequency was accomplished in the composite $0.96Li_3MgNbO_5$-$0.04CaTiO_3$ sintered at 1250°C with ε_r = 19.12, Qxf = 70 814 GHz (at 6.105 GHz), and τ_f = 2.6 ppm/°C.[45]

$Li_3(Mg_{1-x}Zn_x)_4NbO_8$

$Li_3Mg_4NbO_8$ with partial substitution of Zn^{2+} in the Mg^{2+} site was intended to reduce the dielectric loss and contribute to the temperature stability. Specimens with x = 0.02, 0.04, 0.06, and 0.08 in the $Li_3(Mg_{1-x}Zn_x)_4NbO_8$ were sintered in the 1050–1150°C range utilizing the stack-firing method (similar to the use of the powder bed procedure) to avoid Li loss. The bulk density and ε_r were higher for sintering at 1075°C and x = 0.04; the Qxf value reached 121 157 GHz and τ_f −8.23 ppm/°C.[46]

(1-x) Li_2TiO_3 - x $Li_3Mg_2NbO_6$

The composites had their dielectric properties studied for $0.02 \leq x \leq 0.08$ after sintering in the 1200–1300°C range. The rock salt structure was identified in all compositions. The crystalline structure changed gradually from monoclinic to cubic as the fraction of $Li_3Mg_2NbO_6$ increased. The optimal dielectric properties were obtained for sintering at 1250°C and x = 0.04, with ε_r = 19.12, Qxf = 70 814 GHz (at 6.105 GHz), and τ_f = 2.6 ppm/°C.[47] In this particular case and other examples cited here, the production of a composite ceramic intended to adjust the temperature coefficient of the resonant frequency to near-zero values by the formation of a composite with opposite values of τ_f.

$Li_2Ti_{1-x}(Mg_{1/3}Nb_{2/3})_xO_3$ ($0.1 \leq x \leq 0.35$)

Partial substitution of $(Mg_{1/3}Nb_{2/3})^{4+}$ for Ti^{4+} in the Li_2TiO_3 allowed adjusting τ_f to near-zero along with an increase in the Qxf value after sintering at 1170°C. The optimal dielectric properties were obtained for x = 0.25 in $Li_2Ti_{1-x}(Mg_{1/3}Nb_{2/3})_xO_3$ with ε_r ~19.6, Qxf ~109 770 GHz, and τ_f ~1.2 ppm/°C.[48] In a subsequent work,[49] the $Li_2Ti_{0.75}(Mg_{1/3}Nb_{2/3})_{0.25}O_3$ ($LTMN_{0.25}$) composition was mixed with 2 wt.% V_2O_5 or 1 wt.% 0.4 B_2O_3-0.6 CuO (BC) aiming to reduce the sintering temperature of $LTMN_{0.25}$ to near 900°C. Specimens containing V_2O_5 were sintered in the 890–920°C range and co-fired with Al powder at 910°C, while the sintering temperatures of specimens with BC sintering aid were 860–890°C with co-firing at 870°C. Both sintering aids helped to decrease the sintering temperature below the melting point of silver (961°C) giving rise to dense microstructures, and with no diffusion of silver. The optimal dielectric properties (ε_r ~19.9, Qxf ~60 950 GHz, and τ_f ~ −6.1 ppm/°C) were obtained for 1 wt.% BC sintering at 870°C/2 h. A prototype dielectric resonator antenna fabricated with $LTMN_{0.25}$ −0.6 CuO-0.4 B_2O_3 revealed good performance resonating at 10.02 GHz with a bandwidth ~175 MHz.[49]

$Li_5ZnSnNbO_8$

This ceramic, sintered at 1250°C/4 h, exhibited rock salt structure without secondary phases. Overfiring resulted in abnormal grain growth and porosity, due to Li loss. The optimal dielectric properties were: ε_r = 17.17, Qxf = 51 519 GHz, and τ_f = −28.2 ppm/°C.[50]

25783270, 0, Downloaded from https://ceramics.onlinelibrary.wiley.com/doi/10.1002/ces2.10201 by CAPES, Wiley Online Library on [19/01/2024]. See the Terms and Conditions (https://onlinelibrary.wiley.com/terms-and-conditions) on Wiley Online Library for rules of use; OA articles are governed by the applicable Creative Commons License

(1-x) [$Li_2Ti_{0.98}Mg_{0.02}O_{2.96}F_{0.04}$-1 wt.% Nb_2O_5] - x $Li_3Mg_2NbO_6$ ($LTMN_{0.02}$-LMN), 0 ≤ x ≤ 0.1)

The complex composition was sintered in the 1210–1250°C range. Single-phase with rock salt structure was obtained for all compositions. The addition of LMN was carried out to obtain a near-zero τ_f without loss of the other dielectric characteristics. A suitable sintering temperature of 1220°C resulted in high relative densities (~96%). Values of the dielectric properties were $\varepsilon_r = 18.1$, Qxf = 105 661 GHz, and $\tau_f = 1.3$ ppm/°C for x = 0.08.[51]

$Li_2Mg_3Ti_{1-x}(Zn_{1/3}Nb_{2/3})_xO_6$, (0.02 ≤ x ≤ 0.08)

Partial substitution of $(Zn_{1/3}Nb_{2/3})^{4+}$ in the Ti^{4+} site in $Li_2Mg_3TiO_6$ was also studied aiming to improve the Qxf value. The main goal was to produce a dielectric ceramic suitable for microstrip antenna application. Sintering experiments were carried out in the 1260–1360°C range. The bulk density increased with increasing x. The optimal properties were obtained for x = 0.08, sintered at 1285°C with $\varepsilon_r = 13.28$, Qxf = 168 911 GHz, and $\tau_f = -42.88$ ppm/°C.[52]

$Li_2Ti_{0.85}(Mg_{1/3}Nb_{2/3})_{0.15}O_3$

Attempts to stabilize the temperature coefficient of resonant frequency have been made by means of a trilayer composition $Li_2Ti_{0.85}(Mg_{1/3}Nb_{2/3})_{0.15}$ O_3/$MgTiO_3$/ $Li_2Ti_{0.85}(Mg_{1/3}Nb_{2/3})_{0.15}O_3$ ceramic. The dielectric properties obtained were: $\varepsilon_r = 18.4$, Qxf = 85 000 GHz, and $\tau_f = -3.8$ ppm/°C (25–105°C), $\tau_f = 4.0$ ppm/°C (−40 to 25°C).[53]

(1−m) Li_2TiO_3 - m $Zn_3Nb_2O_8$ (m = 0.1, 0.16, 0.2, 0.3)

Ceramics sintered at 1100°C formed a solid solution with diffraction peaks characteristic of $Li_2ZnTi_3O_8$. The $Zn_3Nb_2O_8$ with negative τ_f, relatively high Qxf value, and low sintering temperature was selected to tune the τ_f value of Li_2TiO_3. The average grain size increased from 10 to 23 μm when m increased from 0.1 to 0.3. For m = 0.16, optimum values of the dielectric properties were obtained with ε_r ~18.05, Qxf = 25 791 GHz, and τ_f ~ −6.09 ppm/°C.[54]

$Li_4Mg_2NbO_6F$

LiF was added to lithium niobates to reduce the sintering temperature, due to its relatively low melting point (845°C). Moreover, the substitution of F^- into O^{2-} sites may reduce the oxygen bond strength. The specimens were sintered in the 850–950°C range. The relative density achieved high values (≥ 97.5%) at 900°C. The optimal microwave dielectric properties were obtained after sintering at 900°C: ε_r ~15.53, Qxf = 93 300 GHz, and τ_f ~ −39.8 ppm/°C.[55]

$Li_6MgTiNb_{1-x}V_xO_8F$ (0 ≤ x ≤ 0.08)

The $Li_6MgTiNbO_8F$ composition sintered at 1175°C with cubic rock salt structure exhibited Qxf = 105 700 ± 1600 GHz. It was found that Qxf values varied according to the density and the average grain size. The substitution of V^{5+} for Nb^{5+} decreased the sintering temperature while improving the relative density and relative permittivity. The $Li_6MgTiNb_{0.98}V_{0.02}O_8F$ composition sintered at 850°C/4 h showed $\varepsilon_r = 18.14 \pm 0.05$, Qxf = 58 300 ± 1300 GHz, and $\tau_f = -42.66 \pm 0.33$ ppm/°C.[56]

$Li_7(Nb_{1-x}Ti_x)_2O_{8-x}F$ (0 ≤ x ≤ 0.10)

Partial substitution in the Nb^{5+} site for Ti^{4+} was studied in a series of compounds sintered in the 675–950°C range. Sintering at 900°C yielded a minor fraction of Li_3NbO_4 secondary phase. Further increase of the sintering temperature increased the fraction of the secondary phase, which was attributed to lithium and fluorine volatilization; the Li_7NbO_8F composition sintered at 900°C showed $\varepsilon_r = 16.98$, Qxf = 73 600 GHz, and $\tau_f = -41.6$ ppm/°C; $Li_7(Nb_{0.96}Ti_{0.04})_2O_{7.96}F$ ceramics sintered at 725°C/4 h showed a fine microstructure, well-suited with Ag powders, with $\varepsilon_r = 17.54$, Qxf = 38 800 GHz, and $\tau_f = -44.8$ ppm/°C.[57]

(1-x) $Li_{5.5}Nb_{1.5}O_6F$ - x $Ba_3(VO_4)_2$

Composite ceramics with x = 0, 0.15, 0.20, 0.25, and 0.30 were sintered in the 825–925°C range. Lithium niobate oxyfluoride, $Li_{5.5}Nb_{1.5}O_6F$, exhibited a single-phase rock salt structure. The τ_f value increased continuously with increasing barium vanadate content. The composite ceramic with x = 0.25 sintered at 825°C achieved $\varepsilon_r = 16.68$, Qxf = 55 800 GHz, and $\tau_f = -1.7$ ppm/°C.[58]

$Li_3Mg_4NbO_8$

The composition with orthorhombic structure was sintered in the 1075–1175°C range. This composition exhibited a partially ordered rock salt superstructure. Maximum density was achieved after sintering at 1150°C. The dielectric properties were: $\varepsilon_r = 13.8$, Qxf = 103 400, and $\tau_f = -36$ ppm/°C.[59]

2.2.5 | Compositions without lithium

In parallel with Li-based compositions, several ceramics without lithium were investigated. Extensive research work has been conducted on the dielectric properties of niobate-based ceramics.

$ZnZrNb_2O_8 + Li_2CO_3–B_2O_3–Bi_2O_3–SiO_2$ (LBBS)

The LBBS, a boron-based glass sintering aid, was used with contents varying from 0.5 to 3.0 wt.% to sinter

25783270, 0, Downloaded from https://ceramics.onlinelibrary.wiley.com/doi/10.1002/ces2.10201 by CAPES, Wiley Online Library on [19/01/2024]. See the Terms and Conditions (https://onlinelibrary.wiley.com/terms-and-conditions) on Wiley Online Library for rules of use; OA articles are governed by the applicable Creative Commons License

pure-phase $ZnZrNb_2O_8$. The sintering aid allowed densification at relatively low temperatures. No secondary phases were detected by X-ray diffraction. In addition, LBBS significantly influenced the cell volume and NbO_6 octahedral distortion and, consequently, the dielectric properties. The compound with 0.75 wt.% LBBS sintered at 950°C had $\varepsilon_r = 27.1$, Qxf = 54 500 GHz, and $\tau_f = -48.7$ ppm/°C, besides chemical compatibility with silver electrodes.[60]

$ZnZrNb_2O_8$ + x wt.% LiF, MgF_2, CuO (0.00 ≤ x ≤ 0.10), and $Zn_{1-x}Cu_xZrNb_2O_8$ (0.000 ≤ x ≤ 0.050)

Small amounts of LiF, MgF_2, and CuO were added as sintering aid. The additives significantly improved the dielectric properties of $ZnZrNb_2O_8$. Relevant properties were obtained for CuO additions: ε_r was found to depend on sample density. Doping with CuO promoted grain growth and decrease of the dielectric loss, with a consequent increase of the Qxf value. For x = 0.06, $\varepsilon_r = 27.404$, Qxf = 74 213 GHz, and $\tau_f = -52.779$ ppm/°C; for x = 0.03, $\varepsilon_r = 27.448$, Qxf = 72 520 GHz, and $\tau_f = -53.143$ ppm/°C.[61]

(1-x) $ZnNb_2O_6$ - x TiO_2

Different crystalline structures, including columbite, ixiolite, mixtures of ixiolite and rutile, and rutile, were obtained. The main goal was to tune ε_r and τ_f values with TiO_2 addition. The columbite structure can be interpreted as an ordered superstructure, and the introduction of TiO_2 into the crystalline structure resulted in a disordered system, with a consequent decrease of the Qxf value. The microwave dielectric properties were found to be primarily influenced by the crystalline phase rather than the chemical composition. The optimal properties were achieved for x = 0.5, where the structure was fully disordered, with $\varepsilon_r = 34.3$, Qxf = 42 500 GHz, and $\tau_f = -52$ ppm/°C.[62]

$Zn_{1.01}Nb_2O_6/TiO_2/Zn_{1.01}Nb_2O_6$

The effects of the stacking scheme for sintering and of the TiO_2 content on the microwave dielectric properties of layered architectures were investigated. The reaction layer was found relatively thin (~12 μm). After sintering at 1200°C, τ_f was tuned to ~ + 0.53 ppm/°C, with Qxf ~99 500 GHz and ε_r ~26.8.[63]

(1-x) $Zn_{1.01}Nb_2O_6$ - x TiO_2

Among the dielectric ceramics with columbite structure, $ZnNbO_6$ is known to exhibit good microwave dielectric properties. Similar to Li-based dielectric ceramics, in this case, with an excess of only 0.01 mol of Zn, the Qxf value was improved from 121 000 to 138 000 GHz; for x = 0.6, the dielectric properties were: $\varepsilon_r = 47.43$, Qxf ≥ 12 300 GHz, and $\tau_f = +13.9$ ppm/°C.[64]

$ZnTiNb_2O_8$ - x LBSCA [x (wt.%) = 0, 0.2, 0.4, 0.6, 0.8, 1]

The LBSCA sintering aid was added to lower the sintering temperature of $ZnTiNb_2O_8$; a secondary phase ($ZnNb_2O_6$) was detected by X-ray diffraction; ceramics with x = 0.4 sintered at 950°C/3 h showed $\varepsilon_r = 33.826$, Qxf = 49 143 GHz, and $\tau_f = -57.59$ ppm/∘C.[65]

$ZnTiNb_2O_8$ (ZTN)

This dielectric ceramic was prepared from $ZnNb_2O_6$ and TiO_2 nanopowders prepared by high-energy ball milling. Pure ixiolite $ZnTiNb_2O_8$ ceramics with a relative density of up to 97% were obtained after sintering in the 975–1050°C range. The optimal dielectric properties were: $\varepsilon_r = 35.5$, Qxf = 52 500 GHz (at 6.7 GHz), and $\tau_f = -60.8$ ppm/°C.[66]

x $Zn_{0.5}Ti_{0.5}NbO_4$ - (1-x) $Zn_{0.15}$ $Nb_{0.3}Ti_{0.55}O_2$, x = 0.0–1.0

The structural evolution with x was thoroughly investigated, and a temperature-stable ceramic, that is, with a small variation of the dielectric properties with the temperature, was obtained for x = 0.516: ε_r ~ 46.11, Qxf ~ 27 031 GHz, and τ_f ~ −1.51 ppm/°C.[67] The temperature coefficient of resonant frequency was tuned by combining a negative value of τ_f ($Zn_{0.5}Ti_{0.5}NbO_4$) with a positive value of τ_f ($Zn_{0.15}$ $Nb_{0.3}Ti_{0.55}O_2$).

(1-x) $ZnTiNb_2O_8$ - x $Zn_{0.17}Nb_{0.33}Ti_{0.5}O_2$ (0.35 ≤ x ≤ 0.75)

The addition of $Zn_{0.17}Nb_{0.33}Ti_{0.5}O_2$ changed τ_f from −39.55 to 54.32 ppm/°C, increased ε_r from ~36.5 to ~51.9, but the Qxf value decreased from 36 914 to 21 077 GHz as x increased. The sintered ceramics exhibited a bimodal distribution of grain sizes and the bulk density was higher for sintering at 1200°C. For x = 0.55, the ceramic sintered at 1200°C/4 h showed $\varepsilon_r = 39.08$, Qxf = 31 384 GHz, and $\tau_f = -6.45$ ppm/°C.[68]

$ZnTiNb_2O_8$ - x $CuTiNb_2O_8$-0.4 wt.% LBSCA (0 ≤ x ≤ 0.4)

To tune the temperature coefficient of resonant frequency, several compositions were prepared by the conventional solid-state synthesis method with polyvinyl alcohol as an organic binder. X-ray diffraction results reveal that increasing x, $ZnTiNb_2O_8$ transforms to $ZnNb_2O_6$, and new phases ($CuTiNb_2O_8$ and Ti_3O_5) were formed at x ≥ 0.3, influencing the microwave dielectric properties. Raman shift explained changes in the dielectric constant. For x = 0.4, high-density samples were obtained, but the Qxf value was comparatively low; this effect was attributed to grain boundaries and grain size. The following dielectric properties were obtained by sintering at 875°C with x = 0.375: $\varepsilon_r = 35.01$, Qxf = 19 449 GHz, and $\tau_f = -0.3$ ppm/°C; the highest Qxf value (~38 711 GHz) was obtained after sintering at 900°C with x = 0.2.[69]

25783270, 0, Downloaded from https://ceramics.onlinelibrary.wiley.com/doi/10.1002/ces2.10201 by CAPES, Wiley Online Library on [19/01/2024]. See the Terms and Conditions (https://onlinelibrary.wiley.com/terms-and-conditions) on Wiley Online Library for rules of use; OA articles are governed by the applicable Creative Commons License

$Zn(Ta_{1-x}Nb_x)_2O_6$ ($0 \le x \le 0.3$)

Partial substitution of Ta in the Nb site was carried out aiming to obtain a high dielectric constant and near-zero temperature coefficient of the resonant frequency ceramic. The ceramics sintered at temperatures ranging from 1200 to 1300°C exhibited an increase in the dielectric constant and a decrease in the quality factor and temperature coefficient, as the value of x increased. The τ_f value decreased to near-zero with increasing x. At frequencies from 6 to 7 GHz and x = 0.3, the dielectric properties were: $\varepsilon_r = 39.81$, Qxf = 42 800 GHz, and $\tau_f = 1.55$ ppm/°C.[70] The microwave dielectric properties of $Zn(Ta_{1-x}Nb_x)_2O_6$ were found to correlate with Ta/Nb-O bond ionicity.

$Zn_{0.997}Cu_{0.003}ZrNb_2O_8 - TiO_2 + ZnO/TiO_2 + CuO/TiO_2 - Zn_{0.997}Cu_{0.003}\ ZrNb_2O_8$

The optimal dielectric properties were attributed to the stable three-layer structure design, and the doping with Cu^{2+} and Zn^{2+} to prevent the reduction of Ti^{4+} to Ti^{3+}. The three-layer ceramics sintered at 1240°C/6 h with 0.05 wt.% TiO_2+ZnO exhibited the dielectric characteristics: $\varepsilon_r = 33.75$, Qxf = 59 000 GHz, and $\tau_f = +2.27$ ppm/°C.[71]

$CaTi_{1-x}(Al_{0.5}Nb_{0.5})_xO_3$ ($0 \le x \le 0.75$)

The ceramics sintered at 1525–1550°C/3 h exhibited orthorhombic structure, bulk density values ≥ 98%, and the grain size ranging from ~9 to ~35 μm. The Qxf value first increased with x, due to the stable perovskite structure, with increased bond strength and covalence, but decreased at x = 0.75. In this case, similar to other reports, the secondary phase was explored to adjust the dielectric properties. An optimal combination of the dielectric properties was found for x = 0.45 with $\varepsilon_r = 55.1$, Qxf = 49 700 GHz, and $\tau_f = 5$ ppm/°C.[72]

$(Zn_{1-x}Ni_x)ZrNbTaO_8$ ($0.02 \le x \le 0.10$)

Single-phase ceramics with wolframite structure were obtained after sintering in the 1130–1200°C range. The relative densities were higher than 95% and the grain size increased with Ni^{2+} addition. Solid solutions with monoclinic structure were found in the whole range of x. The optimal dielectric properties were obtained for x = 0.06 with $\varepsilon_r = 27.88$, Qxf = 128 951 GHz, and $\tau_f = -39.9$ ppm/°C.[73]

$Ni_{0.4}Zn_{0.6}Ti_{(1-x)}Zr_xNb_2O_8$

The doping with Zr was intended to increase the quality factor and to obtain a thermally stable ceramic. The ixiolite structure disappeared when the Zr^{4+} content was higher than 0.2. The Qxf value was found to increase from 32 114 GHz (x = 0.1) to 45 733 GHz (x = 0.3), and the τ_f value changed from −38.1 ppm/°C (x = 0.3) to 3 ppm/°C (x = 0.1). $Ni_{0.4}Zn_{0.6}Ti_{0.7}Zr_{0.3}Nb_2O_8$, sintered at 1120°C/6 h, showed $\varepsilon_r = 29.7$, Qxf = 92 078 GHz, and $\tau_f \sim -38$ ppm/°C.[74]

$(Ti_{0.6}Zr_{0.4})_{0.8}(Zn_{1/3}Nb_{2/3})_{0.2}O_2$

The dielectric properties of the $(Ti_{0.6}Zr_{0.4})_{0.8}(Zn_{1/3}Nb_{2/3})_{0.2}O_2$ ceramic were studied to determine the effects of the residual stress and dislocations on those parameters. The residual stress effect on microwave dielectric loss was reported using high-resolution Raman spectroscopy. It was found that the dielectric loss increases with increasing the residual stress. The ceramics with greater residual stress exhibited much higher dielectric loss, because it increased the vibration anharmonicity of the lattice. The composition sintered at 1200°C achieved $\varepsilon_r = 41.1$, Qxf = 48 230 GHz (at 5.9 GHz), and $\tau_f = -9.7$ ppm/°C.[75]

$La(Nb_{1-x}Ta_x)O_4$ ($0 \le x \le 0.10$)

The ceramic compositions sintered at 1325°C exhibited a single monoclinic fergusonite structure. The evolution of the ε_r value was closely related to that of bond ionicity. The Qxf values showed similar behavior as the lattice energy and τ_f followed the bond energy variation. The optimal dielectric properties were obtained for x = 0.08 with relative density of 98%: $\varepsilon_r = 19.23$, Qxf = 65 653 GHz, and $\tau_f = 3.03$ ppm/°C.[76]

$Ca_4La_2Ti_{5-x}(Mg_{1/3}Nb_{2/3})_xO_{17}$ ($0 \le x \le 4$)

Single-phase ceramics were obtained after sintering in the 1480–1560°C range. The ε_r of sintered ceramics decreased from 71.86 to 35.23, the Qxf value increased from 15 070 to 21 277 GHz, and τ_f varied from 125.2 to −16.7 ppm/°C, with x increasing from 0 to 4. A near-zero $\tau_f \sim -1.62$ ppm/°C was achieved at x = 3 with $\varepsilon_r \sim 40.45$ and Qxf ~19 123 GHz.[77]

$LaTiNbO_6$

Sintering at 1300–1400°C yielded ceramics with monoclinic structure. However, annealing at 1100°C for 0.5–8 h promoted a gradual change to orthorhombic structure. The dielectric parameters were determined for several contents of monoclinic and orthorhombic phases. The values of ε_r and τ_f increased with increasing the amount of orthorhombic phase, whereas Qxf showed the opposite trend. For long annealing times, a pure orthorhombic phase was obtained with the following dielectric properties: $\varepsilon_r = 48.7$, Qxf = 10 018 GHz, and $\tau_f = 69.7$ ppm/°C.[78]

$Mg_{0.5}Zn_{0.5}TiNb_2O_8$

To optimize the dielectric properties of $ZnTiNb_2O_8$, the partial substitution of Mg^{2+} at the Zn^{2+} site was investigated. The composition $Mg_{0.5}Zn_{0.5}TiNb_2O_8$ was sintered at temperatures ranging from 1100 to 1180°C. It was observed

25783270, 0, Downloaded from https://ceramics.onlinelibrary.wiley.com/doi/10.1002/ces2.10201 by CAPES, Wiley Online Library on [19/01/2024]. See the Terms and Conditions (https://onlinelibrary.wiley.com/terms-and-conditions) on Wiley Online Library for rules of use; OA articles are governed by the applicable Creative Commons License

that for sintering temperatures below 1120°C, the quality factor primarily depended on the density. However, for higher sintering temperatures, the quality factor was influenced by the crystal structure, and the temperature coefficient of the resonant frequency τ_f varied from approximately −3.2 to −5.3 ppm/°C as the bond strength of Mg/Zn-O decreased. Typical dielectric properties obtained after sintering at 1120°C were as follows: ε_r = 30.74, Qxf = 66 900 GHz, and τ_f = −4.01 ppm/°C.[79]

$MgZrNb_2O_8$

A single-phase ceramic was obtained after sintering in the 1280−1360°C range; when sintered at T_s < 1340°C, the Qxf value varied mainly according to the relative density; at T_s > 1340°C, the quality factor depended also on the grain morphology. The specimen sintered at 1340°C/4 h, with an average grain size of ∼2 μm, exhibited ε_r = 26, Qxf = 120 816 GHz (at 6.85 GHz), and τ_f = −50.2 ppm/°C.[80]

$MgZr_{0.85}Sn_{0.15}Nb_2O_8$

The ceramics were sintered in the 1220−1340°C range to determine the effect of the sintering temperature on the dielectric properties of this composition. Characteristic wolframite structure was obtained with no trace of secondary phases. The maximum density value was obtained after sintering at 1260°C, the unit cell volume being the lowest. The ε_r value followed the same trend as the total bond ionicity, the Qxf values the total lattice energy, and the τ_f values the total bond energy. Typical microwave dielectric properties obtained at 1260°C were: ε_r = 24.91, Qxf = 94 014 GHz, and τ_f = − 43.93 ppm/°C.[81]

$Mg_{1-x}Ca_xZrNb_2O_8$

A suitable Ca^{2+} concentration was able to increase Nb–O bond ionicity and Nb–O bond lattice energy, contributing to an improvement in the dielectric constant and Qxf value; the τ_f was influenced by the bond valence and thermal expansion coefficient of the Mg–O bond. The introduction of Ca^{2+} promoted changes in the microstructure of ceramics (grain shape and size). For x = 0.04, ε_r = 25.21, Qxf = 116 000 GHz (at 7.17 GHz), and τ_f = −24.4 ppm/°C.[82]

$MgZr_{1-x}Ti_xNb_2O_8$ ($0 \le x \le 0.4$)

The ceramic compositions with organic binder (13 wt.% polyvinyl alcohol) were sintered in the 1240−1340°C range. The addition of Ti^{4+} promoted an increase of the bulk density. The introduction of Ti^{4+} in the crystal lattice reduced the volume of the unit cell and strengthened the bond covalence by changing the atomic distances in the ZrO_6 and NbO_6. The ε_r and Qxf values were considerably improved with Ti addition. Optimal dielectric properties were obtained for x = 0.1 composition sintered at 1320°C: ε_r = 25.72, Qxf = 130 123 GHz (at 7.308 GHz), and τ_f = −46.60 ppm/∘C.[83]

$(Mg_{1/3}Nb_{2/3})_x(Zr_{0.5}Ti_{0.5})_{1-x}O_2$ (x = 0.00, 0.05, 0.10, 0.13, 0.15, and 0.20)

An appropriate amount of $(Mg_{1/3}Nb_{2/3})^{4+}$ was found to increase the temperature stability and to reduce the microwave dielectric loss of $ZrTiO_4$. All specimens were single phase with orthorhombic structure, and relative densities higher than 96%. The average grain size increased from ∼4 to ∼8 μm with increasing $(Mg_{1/3}Nb_{2/3})$ content. The Qxf value increased with increasing the grain size; the ε_r and τ_f values decreased with increasing x. Both parameters were found dependent on the cation-cation distance, as well as on polarizability and relative density. The annealing approach was applied for reducing the intrinsic loss and improving the Qxf value. The optimum microwave dielectric properties were ε_r ∼40.9, Qxf ∼40 217 GHz, and τ_f ∼0.8 ppm/°C, for x = 0.13.[84]

$MgNb_2O_6$ doped with flake Al_2O_3 (0−5 wt.%)

The phase evolution, microstructure, microwave dielectric properties, and mechanical behavior were investigated. Flake Al_2O_3 was used as a second phase to promote good chemical stability and to improve the mechanical properties of $MgNb_2O_6$. The relative density decreased with increasing Al_2O_3 content. X-ray diffraction measurements revealed a secondary phase, characteristic of alumina, for additions higher than 1 wt.%. The ceramics doped with 1.0 wt.% Al_2O_3 exhibited ε_r = 20.1, Qxf = 109 100 GHz, and τ_f = −69 ppm/°C after sintering at 1300°C/4 h.[85]

$(Mg_{1/3}Nb_{2/3})_x(Zr_{0.4}Ti_{0.6})_{1-x}O_2$ (x = 0.05−0.15)

Ceramics were obtained by two-step sintering (heating at 5°C/min to 1350°C/30 min and cooled down at 10°C/min to 1300°C/24 h) aiming to reduce the residual stress and improve the Qxf value; for x = 0.12, the microwave dielectric properties were ε_r ∼ 40.7, Qxf ∼ 41 461 GHz (5 x that of the normal sintering ceramics), and τ_f ∼ 1.23 ppm/°C.[86]

$MgNb_{2-x}V_{x/2}O_{6-1.25x}$

Low-temperature liquid phase sintering was achieved via the nonstoichiometric substitution of vanadium at the niobium site; for x = 0.2, the ceramic sintered at 1030°C/4 h achieved ε_r = 20.5, Qxf = 91 000 GHz, and τ_f = −65 ppm/°C.[87]

$Mg_{0.5}Zr_{0.5}NbO_4$

Single monoclinic phase ceramics were obtained; the evolution of the dielectric properties with sintering temperature followed that of the density. The ε_r value was found to be related to Nb-O bond ionicity, and Qxf was

25783270, 0, Downloaded from https://ceramics.onlinelibrary.wiley.com/doi/10.1002/ces2.10201 by CAPES, Wiley Online Library on [19/01/2024]. See the Terms and Conditions (https://onlinelibrary.wiley.com/terms-and-conditions) on Wiley Online Library for rules of use; OA articles are governed by the applicable Creative Commons License

TABLE 1 Values of sintering temperature T_s (and time, when reported), dielectric constant ε_r, quality factor Qxf, and temperature coefficient τ_f of niobium-based compositions containing lithium.

Composition	Sintering T_s (°C/h)	ε_r	Qxf (GHz)	τ_f (ppm/°C)	Ref.
Pure $Li_3Mg_2NbO_6$	1250	16.8	79 643	−27.2	35
	950	18	51 870	−23	22
$Li_3(Mg_{0.98}Co_{0.02})_2NbO_6$	1300/4	15.22	127600	−3.64	23
$Li_3(Mg_{0.96}Ca_{0.04})_2NbO_6$ + 6 wt.% LiF	1140/6	16.81	122082	−25.8	24
	900/6	15.85	98012	−28.6	24
$Li_3Mg_{1.98}Cu_{0.02}NbO_6$	1100	15.75	92134	−2	10
$Li_3Mg_{1.9}Sn_{0.3}Nb_{0.8}O_6$ $Li_3Mg_{1.6}Sn_{1.2}$ $Nb_{0.2}O_6$	1290/4	15.9	118700	−32.9	26
	1290/4	11.64	83100	3.9	26
$Li_3(Mg_{0.92}Zn_{0.08})_2NbO_6$ + 0.5 wt% (0.17 Li_2O-0.83V_2O_5)	1120/4	17.2	142331	23.2	27
$Li_{3.04}Mg_{1.96}Zn_{0.04}Nb_{0.96}Ti_{0.04}O_6$	1120/4	14	83395	37.2	27
	925/2	16.3	93100	−34.1	28
$Li_3(Mg_{0.95}A_{0.05})_2NbO_6$					
A=Ca^{2+}	1120–1240/4	15.62	96160	−18.47	25
A=Ni^{2+}		15.24	84810	−23.08	25
A=Zn^{2+}		15.39	82170	−18.57	25
A=Mn^{2+}		12.97	52700	−20.13	25
$Li_3Mg_2(Nb_{0.94}Sb_{0.06})O_6$	1150/6	15.79	94487	−24.53	29
$Li_3Mg_2Nb_{1.98}V_{0.02}O_6$	900/4	16	131000	−26	30
$Li_3Mg_2VO_6$	925	15.1	91000	−24	21
$Li_3Mg_2Nb_{0.98}Ta_{0.02}O_6$	1050–1150/4	15.58	113000	−4.5	11
$Li_3Mg_2(Nb_{0.94}Mo_{0.06})$ $O_{6.03}$	1200/6	15.18	116266	−15.71	31
$Li_3Mg_2Nb_{0.94}W_{0.06}O_{6.03}$	1175/6	15.82	124187	18.28	32
$Li_{3.04}Mg_{1.92}Nb_{0.96}Ti_{0.08}$ O_6	1050–1150/4	15.88	131000	−26.8	33
$Li_{3.02}Mg_{1.96}Nb_{0.98}Ti_{0.4}O_6$	1250/4	16.1	128600	−30.4	34
$Li_{3.9}Mg_{0.2}Nb_{0.1}Ti_{1.8}O_6$	1250/4	20.4	90300	2.9	34
$Li_3Mg_2Nb_{0.96}(Li_{1/5}W_{4/5})_{0.04}O_6$	1150/4	~14	114781	~22.3	35
$Li_3Mg_2Nb_{0.96}(Mg_{1/4}W_{3/4})_{0.04}O_6$		~13.8	105879	~21.2	35
$Li_3Mg_2Nb_{0.96}(Al_{1/3}W_{2/3})_{0.04}O_6$		~13.7	102760	~23.1	35
$Li_3Mg_2Nb_{0.96}(Ti_{1/2}W_{1/2})_{0.04}O_6$		~14.2	12838	~21.2	35
$Li_3Mg_2Nb_{0.96}W_{0.04}O_6$		16.8	79643	27.2	35
$Li_{3.06}Mg_2Nb_{0.94}Ti_{0.06}O_6$	1025/4	14.34	154113	−2.17	36
$Li_3Mg_2NbO_6$ + 0.1 wt.% B_2O_3	925/4	14.0	67451	−16.82	37
($Li_3Mg_2NbO_6$–0.1 TiO_2 + 1 wt.% LBBS (Li_2O-B_2O_3-Bi_2O_3-SiO_2)	900/4	16	42648	−1	38
$Li_3Mg_2NbO_6$ (0.5 wt.% MBS)					
MBS = MgO+ 45 B_2O_3+ 13 SiO_2	925/4	14.5	80759	−20.7	39
0.5 wt.% (52.45 Li_2O:31.06 B_2O_3:11.99 SiO_2:2.25 CaO:2.25 Al_2O_3)	925/4	15.16	90557	−16.22	40
$Li_2Ti_{0.98}Mg_{0.02}O_{2.96}F_{0.04}$–1 wt.% Nb_2O_5 (LTMN) + B_2O_3-CuO	790/4	24.44	60754	22.8	43
0.85 Li_3NbO_4−0.15 $CaTiO_3$	1025/4	21.9	24900	5.6	44
Li_3MgNbO_5	1260	16.2	96796	−24.8	45
$Li_3(Mg_{0.96}Zn_{0.04})_4NbO_8$	1075	15.0	121157	−8.23	46
0.96 Li_2TiO_3 - 0.04 $Li_3Mg_2NbO_6$	1250	19.12	70814	2.6	47
$Li_2Ti_{0.75}(Mg_{1/3}Nb_{2/3})_{0.25}O_3$	1150/2	19.6	109770	~1.2	48
$Li_2Ti_{0.75}(Mg_{1/3}Nb_{2/3})_{0.25}O_3$ + 1.0% (0.4 B_2O_3-0.6 CuO	870/2	19.9	60950	−6.1	49

(Continues)

25783270, 0, Downloaded from https://ceramics.onlinelibrary.wiley.com/doi/10.1002/ces2.10201 by CAPES, Wiley Online Library on [19/01/2024]. See the Terms and Conditions (https://onlinelibrary.wiley.com/terms-and-conditions) on Wiley Online Library for rules of use; OA articles are governed by the applicable Creative Commons License

TABLE 1 (Continued)

Composition	Sintering T_s (°C/h)	ε_r	Qxf (GHz)	τ_f (ppm/°C)	Ref.
$Li_5ZnSnNbO_8$	1250/4	17.17	51519	−28.2	50
0.92 [$Li_2Ti_{0.98}Mg_{0.02}O_{2.96}F_{0.04}$-1 wt.% Nb_2O_5] - 0.08 $Li_3Mg_2NbO_6$ ($LTMN_{0.02}$-LMN)	1220	18.1	105661	1.3	51
$Li_2Mg_3Ti_{0.92}(Zn_{1/3}Nb_{2/3})_{0.08}O_6$	1285	13.28	168911	−42.88	52
$Li_2Ti_{0.85}(Mg_{1/3}Nb_{2/3})_{0.15}O_3$	1260/4	18.4	85000	3.8 (25–105°C), 4.0 (−40–25°C)	53
0.84 Li_2TiO_3-0.16 $Zn_3Nb_2O_8$	1100	18.05	25791	−6.09	54
$Li_4Mg_2NbO_6F$	900	15.53	93300	−40	55
$Li_6MgTiNb_{0.98}V_{0.02}O_8F$	850/4	18.14	58300	−42.66	56
Li_7NbO_8F	900	16.98	73600	−41.6	57
$Li_7(Nb_{0.96}Ti_{0.04})_2O_{7.96}F$	725/4	17.54	38800	−44.8	57
(1-x) $Li_{5.5}Nb_{1.5}O_6F$ - x $Ba_3(VO_4)_2$	825	16.68	55800	−1.7	58
$Li_3Mg_4NbO_8$	1075–1175	13.8	103400	−36	59

dominated by the lattice energy and Nb-O bond energy. The ceramics sintered at 1350°C/4 h showed ε_r = 28.6, Qxf = 82 000 GHz, and τ_f = −47 ppm/°C.[88]

$MgTi_{1-x}(Zn_{1/3}Nb_{2/3})_xO_3$ ($0 \le x \le 0.3$)

The quality factor was found to depend on the electronegativity difference and average covalence, the dielectric constant related to molecular polarizability and tolerance factor, and the temperature coefficient strongly correlated with TiO_6 octahedral distortion; the microwave dielectric properties of ε_r = 17.59, Qxf = 211 600 GHz, and τ_f = −50 ppm/°C were obtained when x = 0.12, sintered at 1250°C/4 h.[89]

$Y_{3-x}Al_5Nb_xO_{12+x}$ ($0 \le x \le 0.16$)

A single-phase solid solution of yttrium aluminum garnet structure was observed for $0 \le x \le 0.1$. A secondary phase, $YNbO_4$, was detected for x > 0.1. It was found that the quality factor Qxf was a function of the grain size, and the temperature coefficient τ_f depended on the bond valence of the cations in the octahedra. The dielectric constant ε_r was influenced by density, ionic polarizability, and secondary phase. Doping $Y_3Al_5O_{12}$ with Nb and reducing the Y stoichiometry inhibited secondary phases. For x = 0.1, the composition sintered at 1700°C/6 h showed ε_r ~10.99, Qxf ~280 387 GHz (at 13.5 GHz), and τ_f ~ −34.7 ppm/°C.[90]

Nb_2O_5 in $Y_3Al_5O_{12}$

Four compositions, $Y_3Al_5O_{12}$, $Y_3Al_5O_{12}$ + 1 wt.% Nb_2O_5, $Y_3Al_{4.955}Nb_{0.045}O_{12}$, and $Y_{2.955}Al_5Nb_{0.045}O_{12}$, were prepared to investigate the effects of Nb_2O_5 and non-stoichiometry on the dielectric properties of $Y_3Al_5O_{12}$. The ε_r value was found dependent on the sample density and polarizability; the Qxf value was improved with increasing the grain size, and the τ_f values were closely related to the bond valence of the cations in the AlO_6 octahedron. The optimal dielectric properties were found for Y-deficient composition ($Y_{2.955}Al_5Nb_{0.045}O_{12}$): ε_r ~10.37, Qxf ~ 161 724 GHz, and τ_f ~ −33.8 ppm/°C.[91]

$BaZnP_{2-x}Nb_xO_7$

A moderate amount of Nb^{5+} was found to promote the densification process. The results showed that ε_r was influenced by the density and the secondary phase ($Ba_3Nb_2P_4O_{18}$). The density and full width at half maximum of the Raman vibrational band played a critical role in affecting the Qxf values. Ceramics sintered at 925°C, with x = 0.02, exhibited ε_r = 7.98, Qxf = 60 615 GHz (tan $\delta = 2.18 \times 10^{-4}$; f = 13.21 GHz), and τ_f = −52.93 ppm/°C.[92]

$(Na_{0.5x}La_{1-0.5x})(Nb_{1-x}Mo_x)O_4$ ($0.0 \le x \le 1.0$)

Solid solutions with tetragonal scheelite structure were obtained for $0.4 \le x < 1.0$. The quality factor Qxf was found to be influenced by grain size, porosity, and cleanliness of the grain boundaries. The τ_f value varied with x from ~27 to ~ −59 ppm/°C. Ceramics sintered at 1160°C/2 h and with x = 0.5 exhibited ε_r ~14.5, Qxf ~45 600 GHz, and τ_f ~ −2.4 ppm/°C.[93]

$(Sm_{1-x}Ca_x)(Nb_{1-x}Mo_x)O_4$ ($x = 0.15–0.7$)

Simultaneous substitutions of the A and B cation in $SmNbO_4$ proved to be effective to optimize the dielectric properties. Specimens with x < 0.375 exhibited typical fergusonite-type structure, and the scheelite-type structure for $x \ge 0.375$. The dielectric constant was composition dependent; an optimum microwave dielectric

25783270, 0, Downloaded from https://ceramics.onlinelibrary.wiley.com/doi/10.1002/ces2.10201 by CAPES, Wiley Online Library on [19/01/2024]. See the Terms and Conditions (https://onlinelibrary.wiley.com/terms-and-conditions) on Wiley Online Library for rules of use; OA articles are governed by the applicable Creative Commons License

TABLE 2 Values of sintering temperature T_s (and time, when reported), dielectric constant ε_r, quality factor Qxf, and temperature coefficient τ_f of niobium-based compositions without lithium.

Composition	Sintering T_s (°C/h)	ε_r	Qxf (GHz)	τ_f (ppm/°C)	Ref.
$ZnZrNb_2O_8$ + 0.75 wt.% Li_2CO_3–B_2O_3–Bi_2O_3–SiO_2 (LBBS)	950	27.1	54500	−48.7	60
$ZnZrNb_2O_8$ + 0.06 wt.% LiF, MgF_2, CuO, and $Zn_{0.94}Cu_{0.06}Zr\ Nb_2O_8$	1200–1280/6	27.404	74213	−52.779	61
$ZnZrNb_2O_8$ + 0.03 wt.% LiF, MgF_2, CuO and $Zn_{0.97}Cu_{0.03}ZrNb_2O_8$		27.448	72520	−53.143	
0.5 $ZnNb_2O_6$ - 0.5 TiO_2	1250	34.3	42500	−52	62
$Zn_{1.01}Nb_2O_6/TiO_2/Zn_{1.01}Nb_2O_6$	1200/4	26.8	99500	0.53	63
0.4 $Zn_{1.01}Nb_2O_6$ - 0.6 TiO_2	1100–1250/4	47.43	12300	13.9	64
$ZnTiNb_2O_8$ - 0.4 wt.% LBSCA	950/3	33.826	49143	57.59	65
$ZnTiNb_2O_8$ (ZTN)	975–1050	35.5	52500	−60.8	66
0.516 $Zn_{0.5}Ti_{0.5}NbO_4$ - 0.484 $Zn_{0.15}\ Nb_{0.3}Ti_{0.\ 55}O_2$	1100/4	46.11	27031	−1.51	67
0.45 $ZnTiNb_2O_8$ - 0.55 $Zn_{O.17}Nb_{0\cdot33}Ti_{0\cdot5}O_2$	1200/4	39.08	31384	−6.45	68
$ZnTiNb_2O_8$ - 0.375 $CuTiNb_2O_8$-0.4 wt.% LBSA	875	35.01	19449	−0.3	69
$ZnTiNb_2O_8$ - 0.2 $CuTiNb_2O_8$-0.4 wt.% LBSA	900		38711		
$Zn(Ta_{0.7}Nb_{0.3})_2O_6$	1200–1300	39.81	42800	1.55	70
$Zn_{0.997}Cu_{0.003}ZrNb_2O_8$ – TiO_2 + ZnO/TiO_2 + CuO/TiO_2 – $Zn_{0.997}Cu_{0.003}\ ZrNb_2O_8$	1240/6	33.75	59000	2.27	71
$CaTi_{0.55}(Al_{0.5}Nb_{0.5})_{0.45}O_3$	1525–1550	55.1	49700	5	72
$(Zn_{0.94}Ni_{0.06})ZrNbTaO_8$	1130–1200	27.88	128951	39.9	73
$Ni_{0.4}Zn_{0.6}Ti_{0.7}Zr_{0.3}Nb_2O_8$	1120/6	29.7	92078	∼−38	74
$(Ti_{0.6}Zr_{0.4})_{0.8}(Zn_{1/3}Nb_{2/3})_{0.2}O_2$	1200	41.1	48230	−9.7	75
$La(Nb_{0.92}Ta_{0.08})O_4$	1325	19.23	65653	3.03	76
$Ca_4La_2Ti_2(Mg_{1/3}Nb_{2/3})_3O_{17}$	1480–1560	40.45	19123	∼1.62	77
$LaTiNbO_6$	1300–1400	48.7	10018	69.7	78
$Mg_{0.5}Zn_{0.5}TiNb_2O_8$	1120	30.974	66900	−4.1	79
$MgZrNb_2O_8$	1340/4	26	120816	−50.2	80
$MgZr_{0.85}Sn_{0.15}Nb_2O_8$	1260	24.91	94014	−43.93	81
$Mg_{0.96}Ca_{0.04}ZrNb_2O_8$	1265–1375	25.21	116000	−24.4	82
$MgZr_{0.9}Ti_{0.1}Nb_2O_8$	1320	25.72	130123	−46.60	83
$(Mg_{1/3}Nb_{2/3})_{0.13}(Zr_{0.5}Ti_{0.5})_{0.87}O_2$	1375/4	∼40.9	∼40217	∼0.8	84
$MgNb_2O_6$ doped Al_2O_3 (1 wt.%)	1300/4	20.1	109100	−69	85
$(Mg_{1/3}Nb_{2/3})_{0.12}(Zr_{0.4}Ti_{0.6})_{0.88}O_2$	1350/0.5	∼40.7	∼41461	∼1.23	86
$MgNb_{1.8}V_{0.1}O_{3.5}$	1030/4	20.5	91000	−65	87
$Mg_{0.5}Zr_{0.5}NbO_4$	1350/4	28.6	82000	−47	88
$MgTi_{0.88}(Zn_{1/3}Nb_{2/3})_{0.12}O_3$	1250/4	17.59	211600	−50	89
$Y_{2.9}Al_5Nb_{0.1}O_{12.1}$	1700/6	10.99	280387	−34.7	90
$Y_{2.955}Al_5Nb_{0.045}O_{12}$	1670–1750	10.37	161724	−33.8	91
$BaZnP_{1.98}Nb_{0.02}O_7$	925	7.98	60615	−52.93	92
$(Na_{0.25}La_{0.75})\ (Nb_{0.5}Mo_{0.5})O_4$	1160/2	∼14.5	∼45600	∼−2.4	93
$(Sm_{0.82}Ca_{0.18})\ (Nb_{0.82}Mo_{0.18})O_4$	1460–1540/3	17.1	52800	−1.4	94
$Ba_3Ti_{3.4}(Co_{1/3}Nb_{2/3})_{0.6}Nb_4O_{21}$	950	∼40.99	∼17310	∼−8.62	95

25783270, 0, Downloaded from https://ceramics.onlinelibrary.wiley.com/doi/10.1002/ces2.10201 by CAPES, Wiley Online Library on [19/01/2024]. See the Terms and Conditions (https://onlinelibrary.wiley.com/terms-and-conditions) on Wiley Online Library for rules of use; OA articles are governed by the applicable Creative Commons License

performance for ceramics sintered at 1460–1540°C/3 h was achieved for x = 0.18, with ε_r ~17.1, Qxf ~ 52 800 GHz (at ~ 8.80 GHz), and $\tau_f \sim -1.4$ ppm/°C.[94]

$Ba_3Ti_{4-x}(Co_{1/3}Nb_{2/3})_xNb_4O_{21}$ ($0 \le x \le 12$)

Addition of $(Co_{1/3}Nb_{2/3})^{4+}$ in the Ti site and LBSCA glass along with organic binder as sintering aid were found effective to enhance the dielectric properties of the base ceramic sintered in the 925–975°C. All sintered specimens showed hexagonal lattice along with high density. The optimal dielectric properties were obtained for 0.6 wt.% LBSCA and sintering at 950°C: ε_r ~40.99, Qxf ~ 17 310 GHz, and $\tau_f \sim -8.62$ ppm/°C.[95]

3 | REMARKS

Most of the experiments here reported were performed looking for lowering the sintering temperature, increasing the dielectric constant and the quality factor, and reducing the temperature dependence of the dielectric ceramics. However, accomplishing these objectives is challenging, although a great deal of strong candidates already exists, as summarized in Tables 1 and 2.

As shown in the previous section, among the niobium-based compositions, those containing lithium occupy a prominent position. Another issue worth mentioning is the method of obtaining ceramics using organic binders and sintering aids. Regarding the sintering step, one of the main concerns has been the minimization of component losses. Several works report the addition of a compound, with structural characteristics similar to that of the base composition, but able to exert a compensation effect to obtain a near-zero temperature coefficient. These and other approaches used during the processing of ceramics proved to be effective for the optimization of the dielectric ceramics. Nevertheless, the application of these dielectric materials has been limited due to their relatively low-quality factor (Qxf) values or inadequate thermal stabilities.

Tables 1 and 2 show values of the dielectric constant, the quality factor, and the temperature coefficient of the ceramic compositions reported in this review.

After analyzing the data presented in Tables 1 and 2, Figures 2 and 3 were created to visually illustrate the relationships between different parameters. The observations from Figures 2 and 3 are as follows: (1) there is an inverse correlation between the quality factor and the dielectric constant. Higher quality factors correspond to lower dielectric constants; (2) the temperature coefficient remains within the range of approximately −45 to + 38 ppm/°C for dielectric constants ranging from 12 to 25; and (3) the quality factor falls within the range of

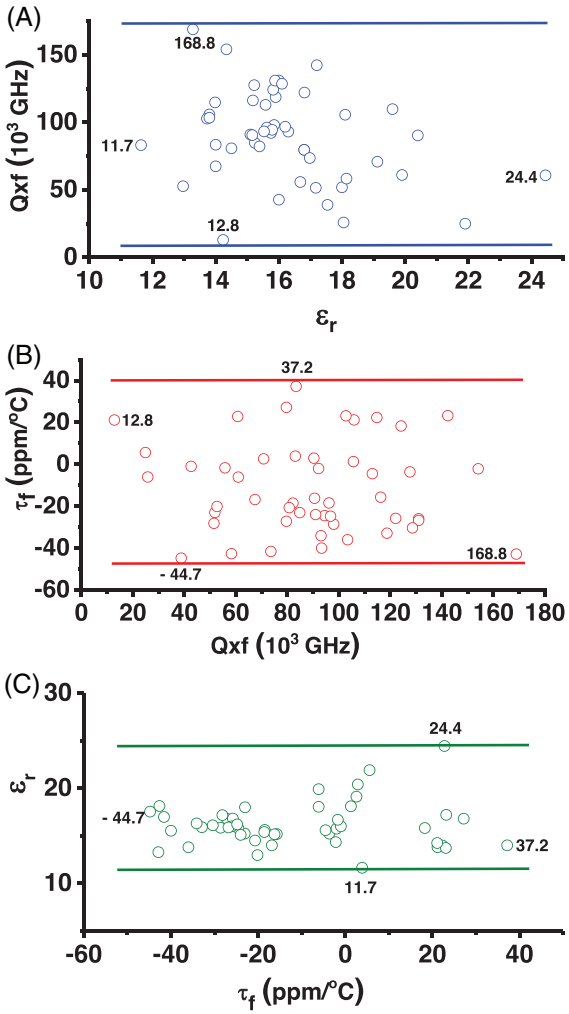

FIGURE 2 Plots of relationships between quality factor, dielectric constant, and temperature factor, after data measured in several lithium magnesium niobate ceramic compounds, collected from Table 1; the lines are guide to the eyes.

approximately 12 000–170 000 GHz. From these figures, it is evident that there is considerable variation in these parameters among different compositions. Therefore, the selection of compositions based on oxides for telecommunication devices by industries depends on various factors, such as the sustainability of material production, material availability and cost, fabrication cost, reproducibility tests and, of course, dielectric properties suitable for telecommunication applications. The presented data and observations may serve as a valuable reference for industries and researchers in making informed decisions regarding the selection and optimization of ceramic compositions for use in telecommunication devices.

Ceramics incorporating niobium in their composition have been successfully developed showing promising dielectric properties, making them suitable candidates for integration into 5G telecommunication devices. Researchers from around the world are actively engaged

25783270, 0, Downloaded from https://ceramics.onlinelibrary.wiley.com/doi/10.1002/ces2.10201 by CAPES, Wiley Online Library on [19/01/2024]. See the Terms and Conditions (https://onlinelibrary.wiley.com/terms-and-conditions) on Wiley Online Library for rules of use; OA articles are governed by the applicable Creative Commons License

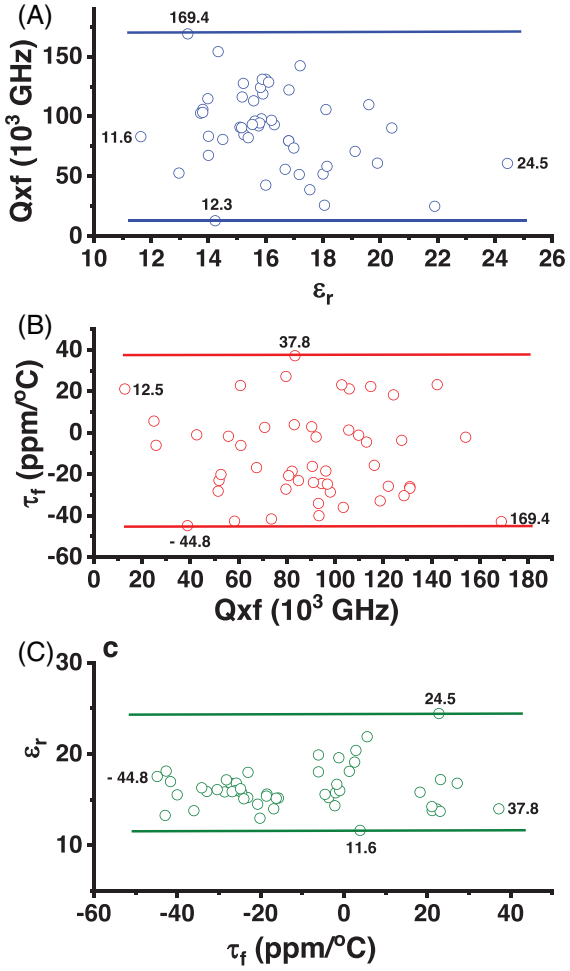

FIGURE 3 Plots of relationships between quality factor, dielectric constant, and temperature factor, after data measured in several lithium magnesium niobate ceramic compounds, collected from Table 2; the lines are guide to the eyes.

in conferences and publishing reports on these ceramics in indexed journals. These publications primarily focus on identifying compositions that exhibit the desired dielectric properties and investigating the relationship between these properties and microstructural features. In addition to the proposed tantalate, titanate, and silicate compositions, this review presents data on more than 80 different niobium-containing compositions, specifically niobates. The main emphasis is on collecting and analyzing data related to the dielectric constant, quality factor, and temperature coefficient, as these parameters play a crucial role in the design and performance of electronic devices for telecommunication applications. The ongoing research and publication of findings in this field highlight the growing interest and efforts to develop advanced niobium-containing ceramics with optimized dielectric properties for the evolving needs of 5G telecommunication systems.

Although the basic properties of the ceramic compositions containing niobium have been investigated, several studies are still needed to demonstrate their reliability for commercialization, such as integration in devices and tests under extreme conditions. The provided data in this paper, in an organized manner, shall serve to feed machine learning efforts for the development of a new generation of Nb-based dielectrics.

AUTHOR CONTRIBUTIONS

Statement of contribution for each author: R. Muccillo (design, collecting references, writing, approval); E.N.S. Muccillo (collecting references, writing).

CONFLICT OF INTEREST STATEMENT

The authors state that there is no conflict of interest.

ORCID

Reginaldo Muccillo https://orcid.org/0000-0002-8598-279X
Eliana N. S. Muccillo https://orcid.org/0000-0001-9219-388X

REFERENCES

1. Hill MD, Cruickshank DB. Ceramic materials for 5G wireless communication systems. Am Ceram Soc Bull. 2019;98:20–25.
2. Hill MD, Cruickshank DB, MacFarlane IA. Perspective on ceramic materials for 5G wireless communication systems. Appl Phys Lett. 2021;118:120501. https://doi.org/10.1063/5.0036058
3. Sebastian MT, Jantunen H. Low loss dielectric materials for LTCC applications: a review. Int Mater Rev. 2008;53:57–90. https://doi.org/10.1179/174328008%D7;277524
4. Gaurav SG. 5G chipset market expected to witness tremendous growth over forecast period 2019–2024. Am Ceram Soc Bull. 2019;98:6.
5. Zhou D, Wang H, Pang L-X, Yao X, Wu X-G. Microwave dielectric characterization of a Li_3NbO_4 ceramic and its chemical compatibility with silver. J Am Ceram Soc. 2008;91:4115–17. https://doi.org/10.1111/j.1551-2916.2008.02764.x
6. Reaney IM, Iddles D. Microwave dielectric ceramics for resonators and filters in mobile phone networks. J Am Ceram Soc. 2006;89:2063–72. https://doi.org/10.1111/j.1551-2916.2006.01025.x
7. Peng R, Li YX, Su H, Lu Y, Chen M, Du W, Liao B. Experiment and calculation: the Li(Zn, Mn)PO_4 solid solution ceramics with low dielectric constant, high quality factor, and low densification temperature. J Alloy Compd. 2020;842:155709. https://doi.org/10.1016/j.jallcom.2020.155709
8. Yang H, Zhang S, Yang H, Wen Q, Yang Q, Gui L, et al. The latest process and challenges of microwave dielectric ceramics based on pseudo phase diagrams. J Adv Ceram. 2021;10:885–932. https://doi.org/10.1007/s40145-021-0528-4
9. Maex K, Baklanov MR, Shamiryan D, Iacopi F, Brongersma SH, Yanovitskaya ZS. Low dielectric constant materials for microelectronics. J Appl Phys. 2003;93:8793–841. https://dx.doi.org/10.1063/1.1567460

25783270, 0, Downloaded from https://ceramics.onlinelibrary.wiley.com/doi/10.1002/ces2.10201 by CAPES, Wiley Online Library on [19/01/2024]. See the Terms and Conditions (https://onlinelibrary.wiley.com/terms-and-conditions) on Wiley Online Library for rules of use; OA articles are governed by the applicable Creative Commons License

10. Wang G, Zhang DN, Xu F, Huang X, Yang Y, Gan G, et al. Correlation between crystal structure and modified microwave dielectric characteristics of Cu^{2+} substituted $Li_3Mg_2NbO_6$ ceramics. Ceram Int. 2019;45:10170–75. https://doi.org/10.1016/j.ceramint.2019.02.066
11. Wang G, Zhang DN, Huang X, Rao Y, Yang Y, Gan G, et al. Crystal structure and enhanced microwave dielectric properties of Ta^{5+} substituted $Li_3Mg_2NbO_6$ ceramics. J. Am Ceram Soc. 2020;103:214–23. https://doi.org/10.1111/jace.16692
12. Coelho R. Physics of dielectrics for the engineer (fundamental studies in engineering). Elsevier; 2012.
13. Nomura S. Ceramics for microwave dielectric resonator. Ferroelectrics. 1983;49:61–70. https://doi.org/10.1080/00150198308244666
14. Hughes H, Iddles DM, Reaney IM. Niobate-based microwave dielectrics suitable for third generation mobile phone base stations. Appl Phys Lett. 2001;79:2952–54. https://doi.org/10.1063/1.1414296
15. Wu H, Davies PK. Influence of non-stoichiometry on the structure and properties of the $Ba(Zn_{1/3}Nb_{2/3})O_3$ microwave dielectrics: I. Substitution of $Ba_3W_2O_9$. J Am Ceram Soc. 2006;89:2239–49. https://doi.org/10.1111/j.1551-2916.2006.01007.x
16. Li M, Feteira A, Mirsaneh M, Lee S, Lanagan MT, Randall CA, et al. Influence of nontoichiometry on extrinsic electrical conduction and microwave dielectric loss of $BaCo_{1/3}Nb_{2/3}O_3$ ceramics. J Am Ceram Soc. 2010;93:4087–95. https://doi.org/10.1111/j.1551-2916.2010.03999.x
17. Paik JH, Nahm S, Bylin JD, Kim MH, Lee HJ. The effect of Mg deficiency on the microwave dielectric properties of $Ba(Mg_{1/3}Nb_{2/3})O_3$ ceramics. J Mater Sci Lett. 1998;17:1777–80. https://doi.org/10.1023/A:1006664310343
18. Yuan LL, Bian JJ. Microwave dielectric properties of the lithium containing compounds with rock salt structure. Ferroelectrics. 2009;387:123–29. https://dx.doi.org/10.1080/00150190902966610
19. Castellanos M, Gard JA, West AR. Crystal data for a new family of phases, $Li_3Mg_2XO_6$:X = Nb, Ta, Sb. J Appl Crystallogr. 1982;15:116–19. https://doi.org/10.1107/S0021889882011522
20. Wang G, Zhang H, Xu F, Huang X, Lai Y, Gan G, et al. Investigation and characterization on crystal structure and enhanced microwave dielectric properties of non-stoichiometric $Li_{3+x}Mg_2NbO_6$ ceramics. Ceram Int. 2018;44:20539–44. https://doi.org/10.1016/j.ceramint 2018. 08.051
21. Wang PL, Zhu M, Chen Y, Xie F, Xiao N, Hou B, et al. Low loss and low temperature sintering of $Li_3Mg_2NbO_6$ ceramics for LTCC applications. Mater Res Express. 2019;6:086313. https://doi.org/10.1088/2053-1591/ab1fb0
22. Zhao LP, Liu P, Sun GQ, Fu ZF. Nanopowders preparation and dielectric properties of low-fired $Li_3Mg_2NbO_6$ ceramics. J Mater Sci: Mater Electron. 2018;29:5873–77. https://doi.org/10.1007/s10854-018-8559-5
23. Xing CF, Bi JX, Wu HT. Effect of Co-substitution on microwave dielectric properties of $Li_3(Mg_{1-x}Co_x)_2NbO_6$ ($0.00 \le x \le 0.10$) ceramics. J Alloy Compd. 2017;719:58–62. https://doi.org/10.1016/j.jallcom.2017.05.139
24. Zhang P, Sun KX, Liu L, Xiao M. A novel low loss and low temperature sintering $Li_3(Mg_{1-x}Ca_x)_2NbO_6$ microwave dielectric ceramics by doping LiF additives. J Alloy Compd. 2018;765:1209–17. https://doi.org/10.1016/j.jallcom.2018.06.217
25. Zhao Y, Zhang P. Microstructure and microwave dielectric properties of low loss materials $Li_3(Mg_{0.95}A_{0.05})_2NbO_6$ (A = Ca^{2+}, Ni^{2+}, Zn^{2+}, Mn^{2+}) with rock-salt structure. J Alloy Compd. 2016;658:744–48. https://doi.org/10.1016/j.jallcom.2015.10.249
26. Zhang X, Zhang X, Fang Z, Xiong Z, Yang H, Zhang S, Tang B. Effects of lattice evolution and ordering on the microwave dielectric properties of tin-modified $Li_3Mg_2NbO_6$-based ceramics. J Phys Chem C. 2020;124:22069–81. https://doi.org/10.1021/acs.jpcc.0c04762
27. Zhang T, Zuo R. Effect of Li_2O–V_2O_5 addition on the sintering behavior and microwave dielectric properties of $Li_3(Mg_{1-x}Zn_x)_2NbO_6$ ceramics. Ceram Int. 2014;40:15677–84. https://doi.org/10.1016/j.ceramint.2014.07.090
28. Ma J, Cheng Q, Zhang Y, LI C, Zhai S, Liu P, Fu Z. B/C site modified $Li_3Mg_2NbO_6$ dielectric properties for microwave application. J Alloy Compd. 2022;905:164256. https://doi.org/10.1016/j.jallcom.2022.164256
29. Zhang P, Wu SX, Xiao M. Effect of Sb^{5+} substitution for Nb^{5+} on crystal structure and microwave dielectric properties for Li_3Mg_2NbO6 ceramics. J Alloy Compd. 2018;766:498–505. https://doi.org/10.1016/j.jallcom.2018.06.347
30. Wang G, Zhang H, Huang X, Xu F, Gan G, Yang Y, et al. Correlations between the structural characteristics and enhanced microwave dielectric properties of V-modified $Li_3Mg_2NbO_6$ ceramics. Ceram Int. 2018;44:19295–300. https://doi.org/10.1016/j.ceramint.2018.07.156
31. Zhang P, Sun KX, Xiao M, Zheng ZT. Crystal structure, densification, and microwave dielectric properties of $LiMg_2(Nb_{(1-x)}Mo_x)O_{6+x/2}$ ($0 \le x \le 0.08$) ceramics. J Am Ceram Soc. 2019;102:4127–35. https://doi.org/10.1111/jace.16286
32. Zhang P, Hao M, Mao X, Sun K, Xiao M. Effects of W^{6+} substitution on crystal structure and microwave dielectric properties of $Li_3Mg_2NbO_6$ ceramics. Ceram Int. 2020;46:21336–42. https://doi.org/10.1016/j.ceramint.2020.05.229
33. Wang G, Zhang D, Li J, Gan G, Rao Y, Huang X, et al. Crystal structure, bond energy, Raman spectra, and microwave dielectric properties of Ti-doped $Li_3Mg_2NbO_6$ ceramics. J Am Ceram Soc. 2020;103:4321–32. https://doi.org/10.1111/jace.17091
34. Zhang X, Fang ZX, Yang HY, Zhao P, Zhang X, Li YP, et al. Lattice evolution, ordering transformation and microwave dielectric properties of rock-salt $Li_{3+x}Mg_{2-2x}Nb_{1-x}Ti_{2x}O_6$ solid-solution system: a newly developed pseudo ternary phase diagram. Acta Mater. 2021;206:116636. https://doi.org/10.1016/j.actamat.2021.116636
35. Zhang P, Hao M, Xiao M. Microwave dielectric properties of $Li_3Mg_2NbO_6$-based ceramics with $(M_xW_{1-x})^{5+}$ (M = Li^+, Mg^{2+}, Al^{3+}, Ti^{4+}) substitutions at Nb^{5+} sites. J Alloy Compd. 2021;853:157386. https://doi.org/10.1016/j.jallcom.2020.157386
36. Zhang P, Sun K, Mao X, Xiao M, Zheng Z. Crystal structures and high microwave dielectric properties in Li^+/Ti^{4+} ions co-doped $Li_3Mg_2NbO_6$ ceramics. Ceram Int. 2020;46:8097–103. https://doi.org/10.1016/j.ceramint.2019.12.036
37. Zhang P, Liao J, Zhao Y, Zhao X, Xiao M. Effects of B_2O_3 addition on the sintering behavior and microwave dielectric properties of $Li_3Mg_2NbO_6$ ceramics. J Mater Sci: Mater Electron. 2017;28:686–90. https://doi.org/10.1007/s10854-016-5575-1
38. Wang G, Zhang H, Liu C, Su H, Li J, Huang X, et al. Low temperature sintering and microwave dielectric properties of novel temperature stable $Li_3Mg_2NbO_6$-0.1 TiO_2 ceramics. Mater

25783270, 0, Downloaded from https://ceramics.onlinelibrary.wiley.com/doi/10.1002/ces2.10201 by CAPES, Wiley Online Library on [19/01/2024]. See the Terms and Conditions (https://onlinelibrary.wiley.com/terms-and-conditions) on Wiley Online Library for rules of use; OA articles are governed by the applicable Creative Commons License

Lett. 2018;217:48–51. https://doi.org/10.1016/j.matlet.2018.01.049
39. Zhang P, Zhao X, Zhao Y. Effects of MBS addition on the low temperature sintering and microwave dielectric properties of $Li_3Mg_2NbO_6$ ceramics. J Mater Sci: Mater Electron. 2016;27:6395–98. https://doi.org/10.1007/s10854-016-4575-5
40. Wang WW, Liu C, Shi L, Wang G, Zhang HY, Xu W, Zhang H. Effects of Li_2O-B_2O_3-SiO_2-CaO-Al_2O_3 glass addition on the sintering behavior and microwave dielectric properties of $Li_3Mg_2NbO_6$ ceramics. Appl Phys A-Mater Sci & Proc. 2019;125:602. https://doi.org/10.1007/s00339-019-2894-0
41. Bian J, Liang Z, Wang L. Structural evolution and microwave dielectric properties of $Li_{(3-3x)}M_{4x}Nb_{(1-x)}O_4$ (M = Mg, Zn: $0 \le x \le 0.9$). J Am Ceram Soc. 2011;94:1447–53. https://doi.org/10.1111/j.1551-2916.2010.04244.x
42. Zhang X, Tang B, Fang Z, Yang H, Xiong Z, Xue LS, et al. Structural evolution and microwave dielectric properties of a novel $Li_3Mg_{2-x/3}Nb_{1-2x/3}Ti_xO_6$ system with a rock salt structure. Inorg Chem Front. 2018;5:3113–25. https://doi.org/10.1039/C8Q/00955B
43. Wang D, Li L, Du M, Zhan Y. A low-sintering temperature microwave dielectric ceramic for 5G LTCC applications with ultralow loss. Ceram Int. 2021;47:28675–84. https://doi.org/10.1016/j.ceramint.2021.07.027
44. Zhou HF, Wang W, Chen XL, Miao Y, Liu XB, Fang L, He F. Sintering behavior, phase evolution and microwave dielectric properties of thermally stable (1-x) Li_3NbO_4 – x $CaTiO_3$ composite ceramic. Ceram Int. 2014;40:2103–7. https://doi.org/10.1016/j.ceramint.2013.07.124
45. Li J, Zhang Z, Tian Y, Ao L, Chen J, Yang A, et al. Crystal structure and microwave dielectric properties of a novel rock-salt type Li_3MgNbO_5 ceramic. J Mater Sci. 2020;55:15643–52. https://doi.org/10.1007/s10853-020-05141-0
46. Zhang P, Tian X, Fan X. Synthesis, sintering and microwave dielectric properties of Zn-doped $Li_3Mg_4NbO_8$ ceramics. J Alloy Compd. 2022;925:166818. https://doi.org/10.1016/j.jallcom.2022.166818
47. Chu X, Gan L, Ren S, Wang J, Ma Z, Jiang J, et al. Low-loss and temperature-stable (1-x) Li_2TiO_3 - x $Li_3Mg_2NbO_6$ microwave dielectric ceramics. Ceram Int. 2020;46:8413–19. https://doi.org/10.1016/j.ceramint. 2019.012.075
48. Guo H-H, Zhou D, Pang L-X, Su J-Z. Influence of $(Mg_{1/3}Nb_{2/3})$ complex substitutions on crystal structures and microwave dielectric properties of Li_2TiO_3 ceramics with extreme low loss. J Materiomics. 2018;4:368–82. https://doi.org/10.1016/j.jmat.2018.09.002
49. Guo H-H, Zhou D, Du C, Wang P-J, Liu W-F, Pang L-X, et al. Temperature stable $Li_2Ti_{0.75}(Mg_{1/3}Nb_{2/3})_{0.25}O_3$-based microwave dielectric ceramics with low sintering temperature and ultra-low dielectric loss for dielectric resonator antenna applications. J Mater Chem C. 2020;8:4690–700. https://doi.org/10.1039/D0TC00326C
50. Jiang Y, Shen Y, Yang J, Fang Z, Zhang X, Zhao P, Tang B. A novel ultra-low loss ceramic $Li_5ZnSnNbO_8$ with a rock salt structure. Mater Chem Phys. 2022;277:125457. https://doi.org/10.1016/j.matchemphys.2021.125457
51. Wang D, Li L, Du M. Ultra-low dielectric loss lithium-based, temperature stable microwave dielectric ceramics. Ceram Int. 2022;48:1394–401. https://doi.org/10.1016/j.ceramint.2021.09.225
52. Zhan Y, Li LX. Low-permittivity and high-Q value $Li_2Mg_3Ti_{1-x}(Zn_{1/3}Nb_{2/3})_x\ O_6$ microwave dielectric ceramics for microstrip antenna applications in 5G millimeter wave. J Alloy Compd. 2021;957:157608. https://doi.org/10.1016/j.jallcom.2020.157608
53. Li L, He X, Yue T, Zhan Y, Du MK. $Li_2Ti_{0.85}(Mg_{1/3}Nb_{2/3})_{0.15}O_3/MgTiO_3/Li_2Ti_{0.85}\ (Mg_{1/3}Nb_{2/3})_{0.15}O_3$ tri-layer co-fired microwave dielectric ceramics: a strategy to suppress non-linear variation of resonant frequency with temperature and achieve a high Q value. Appl Phys Lett. 2022;120:222901. https://doi.org/10.1063/5.0096503
54. Zhang Y, Huang Y, Wang S, Zhang Y. A novel temperature-stable (1−m) Li_2TiO_3 − m $Zn_3Nb_2O_8$ microwave dielectric ceramic. Funct Mater Lett. 2022;15:2250006. https://doi.org/10.1142/S1793604722500060
55. Zhai S, Liu P, Zhang S. A novel high-Q oxyfluoride $Li_4Mg_2NbO_6F$ microwave dielectric ceramic with low sintering temperature. J Eur Ceram Soc. 2021;41:4478–83. https://doi.org/10.1016/j.jeurceramsoc.2021.02.049
56. Zhai S, Liu P, Wu S. Low temperature sintered $Li_6MgTiNb_{1-x}V_xO_8F$ microwave dielectric ceramics with high-quality factor. J Eur Ceram Soc. 2023;43:82–87. https://doi.org/10.1016/j.jeurceramsoc.2022.09.043
57. Zhai S, Liu P. Microwave dielectric properties of rock-salt structured $Li_7(Nb_{1-x}Ti_x)_2O_{8-x}F$ ($0 \le x \le 0.10$) system with low sintering temperature. Ceram Int. 2022;48:28268–73. https://doi.org/10.1016/j.ceramint.2022.06.132
58. Zhai S, Liu P. Temperature stable $Li_{5.5}Nb_{1.5}O_6F$-based microwave dielectric ceramics for LTCC applications. Ceram Int. 2022;48:15951–58. https://doi.org/10.1016/j.ceramint.2022.02.137
59. Yao G, Yan J, Tan J, Pei C, Liu P, Zhang H, Wang D. Structure, chemical bond and microwave dielectric characteristics of novel $Li_3Mg_4NbO_8$ ceramics. J Eur Ceram Soc. 2021;41:6490–94. https://doi.org/10.1016/j.jeurceramsoc.2021.06.029
60. Wang G, Chen Z, Yan H, Xuan T, Wu M, Zhu X, et al. Crystal structure, Raman spectra, and modified dielectric properties of pure-phase $ZnZrNb_2O_8$ ceramics at low temperature. J Am Ceram Soc. 2023;106:1912–20. https://doi.org/10.1111/jace.18892
61. Huang Z, Li L, Qiao J. Trace additive enhances microwave dielectric performance significantly to facilitate 5G communications. J Am Ceram Soc. 2022;105:7426–37. https://doi.org/10.1111/jace.18688
62. Kim D-W, Kim D-Y, Hong KS. Phase relations and microwave dielectric properties of $ZnNb_2O_6$-TiO_2. J Mater Res. 2000;15:1331–35. https://doi.org/10.1557/jmr.2000.0193
63. Zhang J, Luo Y, Yue ZX, Li LT. High-Q and temperature-stable microwave dielectrics in layer cofired $Zn_{1.01}Nb_2O_6/TiO_2/Zn_{1.01}Nb_2O_6$ ceramic architectures. J Am Ceram Soc. 2018;102:342–50. https://doi.org/10.1111/jace.15924342
64. Zhang J, Yue Z, Li L. Effect of TiO_2 on phase composition and microwave dielectric properties of $Zn_{1.01}Nb_2O_6$ ceramics. Ceram Int. 2017;43:S317–20. https://dx.doi.org/10.1016/j.ceramint.2017.05.293
65. Xiang R, Su H, Li Y, Lu Q, Tang X. Effects of LBSCA glass addition on the sintering characteristic and microwave dielectric properties of $ZnTiNb_2O_8$ ceramics. J Mater Sci: Mater Electron. 2020;31:13460–68. https://doi.org/10.1007/s10854-020-03899-2

25783270, 0, Downloaded from https://ceramics.onlinelibrary.wiley.com/doi/10.1002/ces2.10201 by CAPES, Wiley Online Library on [19/01/2024]. See the Terms and Conditions (https://onlinelibrary.wiley.com/terms-and-conditions) on Wiley Online Library for rules of use; OA articles are governed by the applicable Creative Commons License

66. Bafrooei HB, Feizpour M, Sayyadi-Shahraki A, Song KX. High-performance $ZnTiNb_2O_8$ microwave dielectric ceramics produced from $ZnNb_2O_6$-TiO_2 nano powders. J Alloy Compd. 2020;834:155082. https://doi.org/10.1016/j.jallcom.2020.155082
67. Yang H, Zhang S, Yang H, Zhang X, Li E. Structural evolution and microwave dielectric properties of x $Zn_{0.5}Ti_{0.5}NbO_4$ - (1-x) $Zn_{0.15}$ $Nb_{0.3}Ti_{0.55}O_2$ ceramics. Inorg Chem. 2018;57:8264–75. https://doi.org/10.1021/acs.inorgchem.8b00873
68. Zhou G, Wang D, Zhu H, Bian W, Gu H, Zhu H, et al. Effect of $Zn_{0.17}Nb_{0.33}Ti_{0.5}O_2$ on the microwave dielectric properties of $ZnTiNb_2O_8$ ceramics. Ceram Int. 2022;48:6998–7004. https://doi.org/10.1016/j.ceramint.2021.11.257
69. Qian Y, Su H, Tang X, Huang F, Li Y, Zhang Q. Temperature stability of low-temperature fired (1-x) $ZnTiNb_2O_8$-$xCuTiNb_2O_8$ microwave dielectric ceramics. Ceram Int. 2021;47:24823–30. https://doi.org/10.1016/j.ceramint.2021.05.208
70. Xia W-S, Li L-X, Ning P-F, Liao Q-W. Relationship between bond ionicity, lattice energy, and microwave dielectric properties of $Zn(Ta_{1-x}Nb_x)_2O_6$. J Am Ceram Soc. 2012;95:2587–92. https://doi.org/10.1111/j.1551-2916.2012.05231.x
71. Huang Z, Qiao J, Sun N, Chen C, Wang Y, Li L. Enhanced high dielectric characteristics tri-layer structural ceramics for 5G/6G communications. J Am Ceram Soc. 2023;106:1900–1911. https://doi.org/10.1111/jace.18890
72. Hameed I, Liu XQ, Li L, Liu MY, Chen XM. Structure evolution and improved microwave dielectric characteristics in $CaTi_{1-x}(Al_{0.5}Nb_{0.5})_xO_3$ ceramics. J Alloy Compd. 2020;845:155435. https://doi.org/10.1016/j.jallcom.2020.155435
73. Luo WJ, LI LX, Yu S, Guo Q, Zhang B, Sun Z. Effects of structural characteristics on microwave dielectric properties of low-loss $(Zn_{1-x}Ni_x)ZrNbTaO_8$ ceramics. Ceram Int. 2018;44:12414–19. https://doi.org/10.1016/j.ceramint.2018.03.030
74. Huang X, Zhang DN, Wang G, Li J, Gan GW, Zhang HW. Correlation between the structure and modified microwave dielectric characteristics of Zr^{4+} substituted $Ni_{0.4}Zn_{0.6}Ti_{(1-x)}Zr_xNb_2O_8$ ceramics. Ceram Int. 2019;45:20197–201. https://doi.org/10.1016/j.ceramint.2019.06.290
75. Qiao J, Li L, Peng W, Xue T, Du M. The effect of residual stresses and dislocations on microwave dielectric loss in rutile-related $(Ti_{0.6}Zr_{0.4})_{0.8}$ $(Zn_{1/3}Nb_{2/3})_{0.2}O_2$. Ceram Int. 2022;48:239–47. https://doi.org/10.1016/j.ceramint.2021.09.098
76. Xiao M, Wei Y, Gu Q, Zhou Z, Zhang P. Relationships between bond ionicity, lattice energy, bond energy and the microwave dielectric properties of $La(Nb_{1-x}Ta_x)O_4$ (x = 0–0.10) ceramics. J Alloy Compd. 2019;775:168–74. https://doi.org/10.1016/j.jallcom.2018.09.304
77. Chen G-H, Di J-C, Xu H-R, Jiang M-H, Yuan CL. Microwave dielectric properties of $Ca_4La_2Ti_{5-x}(Mg_{1/3}Nb_{2/3})_xO_{17}$ ceramics. J Am Ceram Soc. 2012;95:1394–97. https://doi.org/10.1111/j.1551-2916.2011.05004.X
78. Zhan J, Zuo R. A novel self-composite property-tunable $LaTiNbO_6$ microwave dielectric ceramic. Mater Res Bull. 2016;83:568–72. https://doi.org/10.1016/j.materresbull.2016.07.004
79. Liao Q, Li L, Ding X, Ren X. A new temperature stable microwave dielectric material $Mg_{0.5}Zn_{0.5}TiNb_2O_8$. J Am Ceram Soc. 2012;95:1501–3. https://doi.org/10.1111/j.1551-2916.2012.05148.x
80. Cheng Y, Zuon R, Lv Y. Preparation and microwave dielectric properties of low-loss $MgZrNb_2O_8$ ceramics. Ceram Int. 2013;39:8681–85. https://dx.doi.org/10.1016/j.ceramint.2013.04.048
81. Xiao M, Lou J, Zhang PJ. Characteristics and microwave dielectric properties of low loss $MgZr_{0.85}Sn_{0.15}Nb_2O_8$ ceramics. J Mater Sci-Mater Electron. 2018;29:18311–19. https://doi.org/10.1007/s10854-018-9945-8
82. Wang G, Zhang D, Li J, Shi L, Yang Y, Gan G, et al. Structural dependence of microwave dielectric performance of wolframite structured $Mg_{1-x}Ca_xZrNb_2O_8$ ceramics: crystal structure, microstructure evolution, Raman analysis and chemical bond theory. J Eur Ceram Soc. 2021;41:3445–51. https://doi.org/10.1016/j.jeurceramsoc.2021.01.033
83. Zhang X, Liu C, Shi L, Xu W, Zhang H, Zeng R, Zhang H. Ti^{4+} modified $MgZrNb_2O_8$ microwave dielectric ceramics with an ultra-high quality factor. J Am Ceram Soc. 2021;104:6054–63. https://doi.org/10.1111/jace.17965
84. Li Y, Qiao JI, Li L. Effects of $(Mg_{1/3}Nb_{2/3})^{4+}$ substitution on the temperature-stable and low-loss $(Mg_{1/3}Nb_{2/3})x(Zr_{0.5}Ti_{0.5})_{1-x}O_2$ microwave dielectric ceramics. Ceram Int. 2022;48:6850–58. https://doi.org/10.1016/j.ceramint.2021.11.237
85. Wang S, Yang A, Jiang S, Peng H, Yao X, Lin H. Significantly enhanced mechanical strength of $MgNb_2O_6$ microwave dielectric ceramics with high Q values. Ceram Int. 2022;48:21084–89. https://doi.org/10.1016/j.ceramint.2022.03.023
86. Qiao J, Li L. Structural, residual stress and sintering schedule studies on $(Mg_{1/3}Nb_{2/3})_x(Zr_{0.4}Ti_{0.6})_{1-x}O_2$ microwave ceramics. Mater Lett. 2022;309:131369. https://doi.org/10.1016/j.matlet.2021.131369
87. Wang S, Li L, Wang X. Low-temperature firing and microwave dielectric properties of $MgNb_{2-x}V_{x/2}O_{6-1.25x}$ ceramics. Ceram Int. 2022;48:199–204. https://doi.org/10.1016/j.ceramint.2021.09.094
88. Li J, Zhu J, Wang G. Correlation between crystal structure and enhanced microwave dielectric characteristics of wolframite-structure $Mg_{0.5}Zr_{0.5}NbO_4$ ceramics. Ceram Int. 2022;48:15261–67. https://doi.org/10.1016/j.ceramint.2022.02.058
89. Li B, Lai Y, Zeng Y, Yang F, Huang F, Yang X, et al. Structure and microwave dielectric properties of $(Zn_{1/3}Nb_{2/3})^{4+}$ co-substituted $MgTiO_3$ ceramic. Mater Sci Eng B. 2022;276:115572. https://doi.org/10.1016/j.mseb.2021.115572
90. Zhou M, Chen H, He Y, Zhou G, Zhang X, Zhang S, Tang B. Phase composition, crystal structure, and microwave dielectric properties of Nb-doped and Y-deficient yttrium aluminum garnet ceramics. J Eur Ceram Soc. 2022;42:5705–11. https://doi.org/10.1016/j.jeurceramsoc.2022.06.015
91. Zhou M, Chen H, Zhou G, He Y, Zhang S, Tang B. Co-effects of Nb_2O_5 and stoichiometric deviations on the microwave dielectric properties of $Y_3Al_5O_{12}$. Ceram Int. 2022;48:18651–57. https://doi.org/10.1016/j.ceramint.2022.03.137
92. Huang F, Su H, Zhang Q, Wu X, Jing Y, Li Y, Tang X. The lattice vibration and microwave dielectric properties of $BaZnP_{2-x}Nb_xO_7$ ceramics for microwave substrates. J Am Ceram Soc. 2022;105:7455–66. https://doi.org/10.1111/jace.18695
93. Pang L, Wang X, Zhou D, Fang Z, Tian X, Liu W, et al. Microwave dielectric properties and vibrational spectra of $(Na_{0.5x}La_{1-0.5x})$ $(Nb_{1-x}Mo_x)O_4$ ceramics with scheelite structures. J Eur Ceram Soc. 2022;42:5726–30. https://doi.org/10.1016/j.jeurceramsoc.2022.05.074

25783270, 0, Downloaded from https://ceramics.onlinelibrary.wiley.com/doi/10.1002/ces2.10201 by CAPES, Wiley Online Library on [19/01/2024]. See the Terms and Conditions (https://onlinelibrary.wiley.com/terms-and-conditions) on Wiley Online Library for rules of use; OA articles are governed by the applicable Creative Commons License

94. Wu F, Zhou D, Du C, Xu D-M, Li R-T, Shi Z-Q, et al. Design and fabrication of a satellite communication dielectric resonator antenna with novel low loss and temperature-stabilized $(Sm_{1-x}Ca_x)$ $(Nb_{1-x}Mo_x)O_4$ (x = 0.15−0.7) microwave ceramics. Chem Mater. 2023;35:104–15. https://doi.org/10.1021/acs.chemmater.2c02663
95. Wu X, Jing Y, Li Y, Su H. Developing high performance, low temperature sintering and temperature stable *K*40 material in Co_2O_3/Nb_2O_5-modified $Ba_3Ti_4Nb_4O_{21}$ microwave dielectric ceramics for 5G-LTCC communication devices. J Alloy Compd. 2023;962:171163. https://doi.org/10.1016/j.jallcom.2023.171163

How to cite this article: Muccillo R, Muccillo ENS. Ceramic compositions for 5G devices containing niobium: A survey. Int J Ceramic Eng Sci. 2024;e10201. https://doi.org/10.1002/ces2.10201

25783270, 0, Downloaded from https://ceramics.onlinelibrary.wiley.com/doi/10.1002/ces2.10201 by CAPES, Wiley Online Library on [19/01/2024]. See the Terms and Conditions (https://onlinelibrary.wiley.com/terms-and-conditions) on Wiley Online Library for rules of use; OA articles are governed by the applicable Creative Commons License